The role of glycogen synthase kinase 3β in adhesion-dependent survival signalling in human oesophageal squamous cell carcinoma

by

Lauren Crooks

791844

Dissertation

Submitted in fulfilment of the requirements for the degree

Master of Science

in

Molecular and Cell Biology

Faculty of Science, University of the Witwatersrand, Johannesburg, South Africa

Supervisor: Professor R Veale

February 2020

i. DECLARATION

I declare that this dissertation is my own, unaided work. It is being submitted for the Master of Science at the University of the Witwatersrand, Johannesburg. It has not been submitted before for any degree or examination at any other University.

Lauren Crooks

22nd day of May 2020

ii. ABSTRACT

Glycogen synthase kinase 3β (GSK3β) has been shown to have more predicted substrates than any other kinase, and thus is suggested to be involved in the regulation of almost every cellular process, however; the interrelationship between GSK3β and its interactors in signalling pathways remains poorly elucidated. Unsurprisingly, dysregulation of GSK3β has been observed in a number of pathological conditions, including cancer. Interestingly, GSK3β is constitutively active under normal conditions, but phosphorylation at Ser-9 leads to inhibition of its activity. The regulation of GSK3β appears complex, and its role in cancer cell survival appears contradictory. This research investigates the role of GSK3β in survival signalling in human oesophageal squamous cell carcinoma (HOSCC), and elucidated that both inactive and active phosphorylated forms are present and differentially regulated. However, it was found that the inactive form of GSK3β contributed notably to enhanced cancer cell survival through diminishing cleaved caspase 3, the executioner caspase of cell death in the form of apoptosis. Furthermore, inactive GSK3β increased proliferation and viability in HOSCC, suggesting inactive GSK3β may be critical in facilitating selective growth advantages in HOSCC. In addition to observing the role of GSK3β on intracellular signalling, the role of GSK3β on adhesion-mediated communication was elucidated. HOSCC appear highly dependent on a dynamic extracellular environment, therefore communication between the cancer cell and surrounding extracellular matrix (ECM) remains indispensible to the progression of the disease. It was found that β1 integrin receptors are present at high levels in HOSCC and are positively regulated by inactive GSK3β. Consequently, a signalling axis between β1 integrin receptors and GSK3β exists in HOSCC and functions in the maintenance of survival and the highly aggressive nature of the malignancy.

iii. CONFERENCE OUTPUTS

Crooks L, and Veale R (2019). The role of glycogen synthase kinase 3β in adhesion-dependent survival signalling in human oesophageal squamous cell carcinoma. Poster presentation at the Molecular Biosciences Research Thrust, University of the Witwatersrand, 28 November 2019.

iv. ACKNOWLEDGEMENTS

I would like to acknowledge and thank my supervisor, Professor R Veale, for his consistent advice, patience, guidance, and support, without which, bringing this research to fruition would not have been possible.

Thank you to Sabeeha Mahomed for all of her assistance with tissue culture and general lab maintenance, as well as for always being good company.

Thank you to my friends and family for their endless support and understanding throughout this degree. Particularly my mother, for being consistently present, always there regardless of how arduous this journey may have been at times. Thank you to my father, ever curious to hear about my research and for only ever being a phone call away.

I would also like to acknowledge and thank the Wits Postgraduate Merit Award and the National Research Foundation for their financial support and funding.

v. TABLE OF CONTENTS

vi. LIST OF FIGURES

vii. LIST OF TABLES

viii. LIST OF ABBREVIATIONS AND SYMBOLS

AP-1	activator protein 1
APAF-1	apoptotic protease activating factor 1
Bak	Bcl-2 homologous antagonist/killer
BAX	Bcl-2-associated X protein
Bcl-2	B cell lymphoma-2
Bfl-1	Bcl-2-related protein A1
BH	Bcl-2 homology
Bid	BH-3 interacting-domain death agonist
Bim	Bcl-2-like protein 11
BSA	bovine serum albumin
CAD	caspase-activated DNase
cAMP	cyclic AMP
CN	collagen type I
CRE	cAMP response element
CREB	cAMP response element-binding protein
COX2	cyclooxygenase-2
DISC	death-inducing signalling complex
DMEM	Dulbecco's Modified Eagle's Medium
ECM	extracellular matrix
EGFR	epidermal growth factor receptor
ER	endoplasmic reticulum
FADD	fas-associated protein with death domain
FAK	focal adhesion kinase
FasL	first apoptosis signal ligand
FasR	first apoptosis signal ligand receptor

FCS	foetal calf serum
FN	fibronectin
GSK3β	glycogen synthase kinase 3β
HOSCC	human oesophageal squamous cell carcinoma
HRP	horseradish peroxidase
ILK	integrin-linked kinase
$iPLA_2$	independent phospholipase A_2
kDa	kilodalton
LEF	lymphoid enhancer binding factor
LEF-1	lymphoid enhancer binding factor 1
MAPK	mitogen-activated protein kinase
Mcl-1	myeloid cell leukemia protein 1
MOMP	mitochondrial outer membrane permeabilisation
MTT	3-(4,5-dimethylthiazol-2-yl)-2,5-diphenyltetrazolium bromide
NF-κB	nuclear factor-κB
NT	untreated
PAGE	polyacrylamide gel electrophoresis
PI3K	phosphatidylinositol 3-kinase
PGE_2	prostaglandin E_2
PKB	protein kinase B
PMSF	phenylmethylsulphonyl fluoride
SDS	sodium dodecyl sulphate
SDS-PAGE	sodium dodecyl sulphate-polyacrylamide gel electrophoresis
SEM	standard error of the mean
SMAC	second mitochondria-derived activator of caspases
TBS	tris-buffered saline
TBS-T	tris-buffered saline with Tween 20

TCA	trichloroacetic acid
TCF	T-cell factor
TNF	tumour necrosis factor
TNFR-1	tumour necrosis factor receptor-1
WHCO	Wits Human Carcinoma of the Oesophagus
XIAP	X-linked inhibitor of apoptosis protein

CHAPTER 1: Introduction and Literature Review

1.1 Adhesion-based signalling is central to the maintenance of normal epithelial cell function and physiology

The maintenance of stabilised cellular interactions is fundamental to the structural and functional integrity of specialised tissue in multicellular organisms by enabling networks of communication and coordination between the diverse cell types required for multicellularity (Trigos *et al.*, 2018). Cell adhesion events are primarily responsible for the establishment of these cellular interactions that drive communication and coordination between the different cell types, and elicit a mechanical and structural role in tissue organisation (Gumbiner, 1996). Particularly, the establishment of the first evolved multicellular organism was determined to be a consequence of the organised and coordinated adhesion between epithelial cells and their adjacent environment, forming cooperative sheets of polarised epithelial cells into a selective barrier separating the internal milieu of the organism from the external environment (Dickinson *et al.*, 2011).

Certainly therefore, adhesion events between epithelial cells are therefore critical for the development and morphogenesis of epithelial cells into specialist tissue. In addition to the structural and mechanical role of cell adhesion in epithelial tissue, cell adhesion events provide the necessary biochemical framework to facilitate the transmission of signals originating in the local extracellular environment into the epithelial cells, ultimately influencing epithelial tissue behaviour and homeostasis (St Johnston and Ahringer, 2010). Central to the relay of these local extrinsically-originating signals into the epithelial cell and subsequent cellular and tissue homeostasis are transmembrane integrin receptors, responsible for the establishment of adhesive contacts of epithelial cells with respective extracellular matrix (ECM) constituents. Consequently, as shown in Figure 1.1, the adhesion between specific ECM ligands in the local extracellular environment to epithelial cells as facilitated by integrin receptors remains indispensible to the homeostatic maintenance of epithelial cells and epithelial tissue as a result of the activation of intracellular signalling pathways (Macara and McCaffrey, 2013).

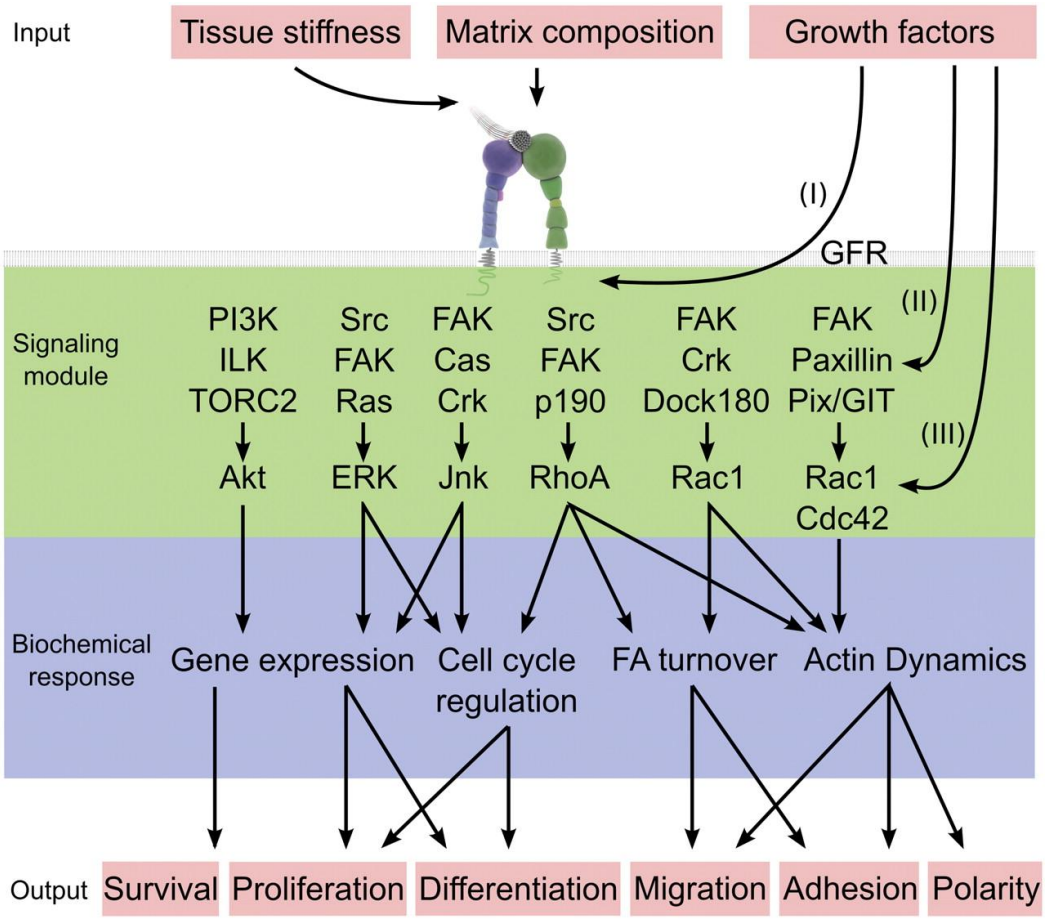

Figure 1.1. Integrin-mediated signalling at the cell-ECM interface modulates cellular homeostasis through the recruitment of intermediates to focal adhesion sites.

Ligation of integrin receptors to ECM constituents results in the clustering of integrin receptors along the cell surface. Subsequently, integrin receptors recruit adaptor and scaffolding molecules to the cytoplasmic side of focal adhesion sites, linking the extracellular environment to intracellular signalling pathways. As a result, cellular processes, such as growth, proliferation, migration, and survival are regulated by linkage of ECM by integrin receptors (Legate and Fässler, 2009).

It is therefore unsurprising that aberrations in cell-ECM communication and, as a consequence, cell adhesion-mediated signalling pathways have been implicated with a number of pathological conditions, such as inflammatory disease, neurological disease, cardiovascular disease, as well as malignant transformation leading to tumourigenesis and the development of cancer (Vanderslice and Woodside, 2006; Liu *et al.*, 2012; Blann and Lip, 2000; Hanahan and Weinberg, 2011).

The development of cancer has been identified to occur as a mechanistically complex and dynamic process, relying on the dysregulation of adhesion-based signalling, as well as specific cues occurring in the local extracellular environment, contributing to proliferative and survival advantages allowing the cancer to progress (Fernald and Kurokawa, 2013). Therefore, the elucidation of the causal adhesion-based signalling pathways contributing to tumour cell survival, and ultimately cancer progression and metastasis, the key interactors involved in these pathways, as well as the influence and role of the constituents of tumour microenvironment and ECM in survival-associated pathways is fundamental to ascertaining the molecular landscape of epithelial malignancies to identify prospective therapeutic strategies in the treatment of these malignancies.

1.2 Dysfunctional integrin signalling contributes to malignant transformation and cancer progression

Adhesion events established between integrin receptors and local extracellular constituents, particularly ECM ligands, are necessary for the appropriate modulation of epithelial cell behaviour and homeostasis. Integrin receptors are able to facilitate homeostasis by not only enabling the cell to respond to alterations in the composition of the local extracellular environment, but by further allowing the cell to modify the existing extracellular environment as a result of the bidirectional functionality of integrin receptors in a process known as inside-out and outside-in signalling, respectively, as represented in Figure 1.2 (Li *et al.*, 2003). Integrin receptors constitute a family of heterodimeric transmembrane proteins composed of non-covalently associated alpha and beta subunits, with extracellular ECM ligand-binding domains and intracellular cytoplasmic tail domains. The ECM ligand specificity of integrin receptors is conferred by the alternate association of the alpha and beta subunits where, in humans specifically, 18 α and 8 β subunits have been identified and associate into 24 possible integrin heterodimer pairs (Humphries, 2006).

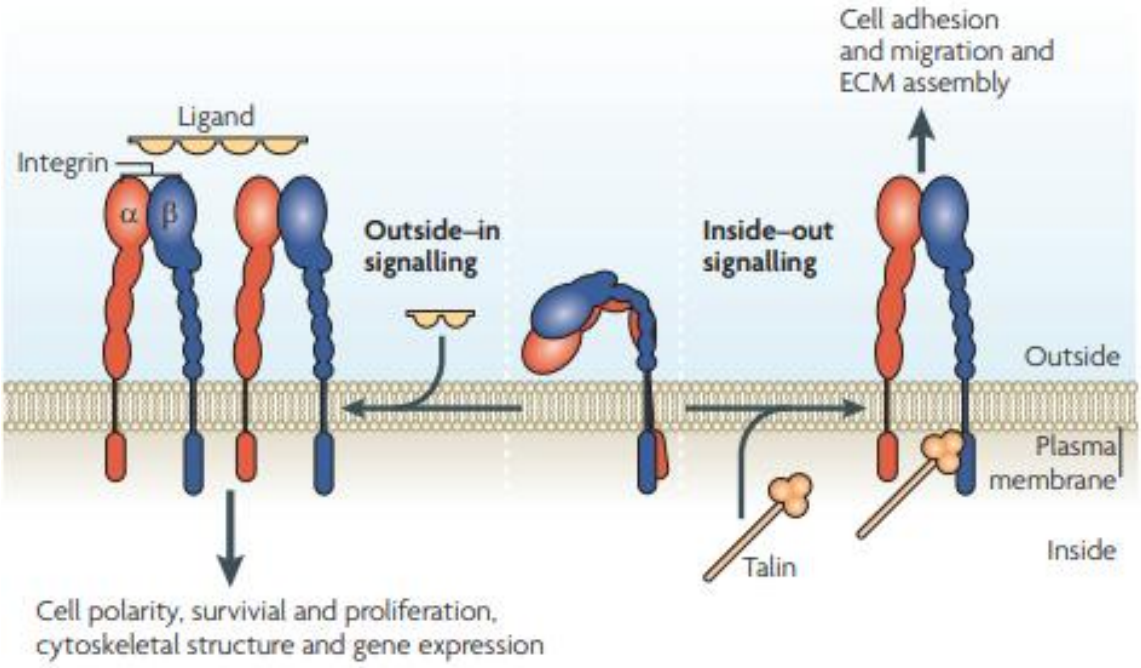

Figure 1.2. Integrin receptors exhibit bidirectional functionality through inside-out and outside-in signalling.

Once activated following the binding of an ECM ligand, integrin receptors cluster along the surface of the cell and recruit adaptor proteins to the cytoplasmic side of the receptor to facilitate intracellular signalling in a process known as outside-in signalling. Conversely, signals originating within the cell can lead to the activation of integrin receptors subsequently resulting in the relay of internal signals to the outside of the cell, modifying the extracellular environment, in a process known as inside-out signalling (Shattil *et al.*, 2010).

Upon binding of ECM ligands to the respective integrin receptors, the integrin receptors cluster along the surface of the cell forming focal adhesion sites which link the extracellular environment to the actin cytoskeleton and downstream interactors. The assembly of these downstream signalling complexes at the cytoplasmic tail domain of integrin receptors during the formation of focal adhesions is necessary for the regulation of signal transduction and cell homeostasis by integrin receptors as integrin receptors lack enzymatic activity (Campbell and Humphries, 2011). Subsequently, intracellular adaptor proteins, such as focal adhesion kinase (FAK) and integrin-linked kinase (ILK) are recruited to focal adhesion sites (Rooney and Streuli, 2011).

The formation of these large multiprotein complexes on the cytoplasmic side of focal adhesions mechanically link the ECM to the actin cytoskeleton, and additionally establish the platforms necessary for the activation of adhesion-based signalling pathways modulated by integrin receptors. As a consequence, the linkage of ECM to the cell as facilitated by integrin receptors and the recruitment of adaptor proteins results in the regulation of a number of cellular processes, including cell growth, proliferation and migration (Rooney and Streuli, 2011). Particularly in epithelial tissue, integrin receptors containing the β1 subunit are the most widely expressed, specifically binding fibronectin, laminin, collagen type-I, and collagen-type IV in the local extracellular environment and are involved in the regulation of a wide range of cellular processes, such as cell survival in addition to their role in mechanical adhesion (Lee and Streuli, 2014). Specifically, normal cells are dependent on the appropriate ligation of ECM ligands to integrin receptors for survival by facilitating cell survival or the initiation of cell death, depending on the local extracellular cues that are probed by the integrin receptors (Frisch and Francis, 1994).

In general, adhesion of integrin receptors with ECM ligands confers survival signals, whereas integrin receptors not bound to ECM promote cell death. Loss of anchorage of cells initiates cell death in the form of anoikis which constitutes a physiologically important mechanism that facilitates the prevention of adhesion of cells detached from ECM to inappropriate locations (Chiarugi, 2008). As such, the appropriate adhesion of integrin receptors to ECM ligands has been associated with tumour suppression, functioning as a natural barrier to cancer development (Macara and McCaffrey, 2013). It is therefore unsurprising that aberrant adhesion between ECM and integrin receptors has been shown to contribute to malignant transformation and cancer progression by eliciting dysfunctional integrin signalling, implicated with aberrations in intracellular signalling pathways (Xu *et al.*, 2017).

In particular, integrin receptors have been shown to modulate tumour cell survival through the regulation of programmed cell death by apoptosis. Integrin receptors have been suggested to contribute to tumour cell survival through a number of downstream mechanisms, including the activation of the nuclear factor-κB (NF-κB) signalling pathway, inactivation of the tumour suppressor p53, as well as increased expression of the pro-survival B cell lymphoma-2 (Bcl-2) (Nam *et al.*, 2013; Martin *et al.*, 2012; Popov *et al.*, 2011). Consequently, dysfunctional integrin signalling, specifically β1 integrin-associated pathways, and the key downstream signalling intermediates in these pathways may be a fundamental mechanism in the evasion of the induction of programmed cell death by apoptosis and enhanced survival in epithelial malignancies.

1.3 The tumour microenvironment and ECM remodelling plays a pivotal role in tumour progression and survival

During malignant transformation and tumour progression, the ECM has been found to experience compositional changes, such as enhanced deposition of ECM components including fibronectin and collagen-type I, as well as increased cross-linking and ECM stiffness. Consequently, these compositional alterations result in modified integrin signalling (Cox and Erler, 2011). The remodelling of ECM as a result of increased deposition of ECM alters the tumour microenvironment, thus disrupting the normal regulation of signalling by integrin receptors by eliciting aberrant cell–ECM communication, as well as altered growth factor signalling (Paszek *et al.*, 2005).

Collagen-type I is a highly abundant constituent of ECM, accounting for the majority of the ECM composition in humans. Collagen-type I is a structural component of the ECM, present in all fibrous tissue due to the triple helix polypeptide chain conformation with a repeating Gly-X-Y sequence (Brodsky and Persikov, 2005). Collagen-type I therefore not only acts in the mechanical support structure for cells and cell–cell anchorage, but has further been associated with tumour development and cancer progression by modification of the ECM as a result of collagen degradation, deposition, and stiffening. Notably, it has been found that enhanced deposition of collagen I results in stiffening of the ECM in breast cancer development and subsequent metastasis (Ramaswamy *et al.*, 2003).

Similarly, fibronectin is a widely expressed component of ECM that is critical in appropriate cell adhesion, growth and differentiation, and has been found to participate in the dysfunction of cell-ECM signalling in malignancies (Pankov and Yamada, 2002). Fibronectin is an

extracellular glycoprotein that exists as a protein dimer, consisting of two nearly identical polypeptide chains (Mao and Schwarzbauer, 2005). Increased deposition of fibronectin has been identified in epithelial malignancies, and is involved in tumour progression by promoting cell growth, migration, invasion and survival (Wang and Hielscher, 2017). As such, ECM constituents and alterations to the ECM architecture significantly influence cancer progression through the dysregulation of integrin signalling pathways.

1.4 Integrin-linked kinase and focal adhesion kinase act as molecular conduits for integrin-mediated survival signalling

As integrin receptors lack enzymatic activity, they rely on the formation of signalling complexes at focal adhesion sites to induce integrin-mediated signalling, illustrated in Figure 1.3. ILK is a 59 kDa Ser/Thr protein kinase that is directly recruited to the cytoplasmic side of focal adhesion sites by the cytoplasmic tail domains of β1 subunit-containing integrin receptors, subsequently facilitating integrin signalling (McDonald *et al.*, 2008). ILK confers a multifunctional capacity that is attributed to several functionally significant domains, although the C-terminal kinase-like domain is principally involved in facilitating integrin-mediated signalling through interacting with β1 and β3 subunit-containing integrin receptors and activating a range of signalling pathways downstream. ILK achieves this function by the phosphorylation of downstream proteins, including protein kinase B (PKB)/Akt and glycogen synthase kinase 3β (GSK3β) in a phosphatidylinositol 3-kinase (PI3K)-dependent manner (Li *et al.*, 2012).

Therefore, ILK participates in the regulation of several cellular processes downstream of integrin ligation to ECM, such as epithelial cell polarity, cell spreading, migration, proliferation, and survival (McDonald *et al.*, 2008). Specifically, ILK phosphorylates and activates PKB/Akt at Ser-473, which regulates the transcription of genes necessary for survival, such as NF-κB target genes (Persad *et al.*, 2000). ILK also directly phosphorylates GSK3β at Ser-9, inhibiting GSK3β and contributing to the modulation of intermediates also involved in cell survival, such as activator protein 1 (AP-1), β-catenin, and cyclic AMP (cAMP) response element (CRE)-binding protein (CREB) (Maydan *et al.*, 2010; Oloumi *et al.*, 2004).

Also recruited to focal adhesion sites to facilitate the generation of integrin signalling platforms is FAK, a 125 kDa tyrosine kinase. Following activation by integrin receptors, FAK experiences autophosphorylation at Tyr-397 and forms a complex with a number of

proteins, including Src and PI3K (Schaller *et al*., 1994; Chen and Guan, 1994). FAK thereby phosphorylates intermediates downstream of integrin perception of ECM in a PI3K-dependent manner, leading to the regulation of cellular processes, including adhesion, migration, differentiation and survival. As with ILK, FAK phosphorylates PKB/Akt and GSK3β downstream (Gao *et al*., 2015). From this, ILK and FAK both act as molecular conduits linking adhesion-based signals to downstream signalling intermediates, such as PKB/Akt and GSK3β, thereby facilitating dysfunctional integrin-mediated signalling in epithelial malignancies.

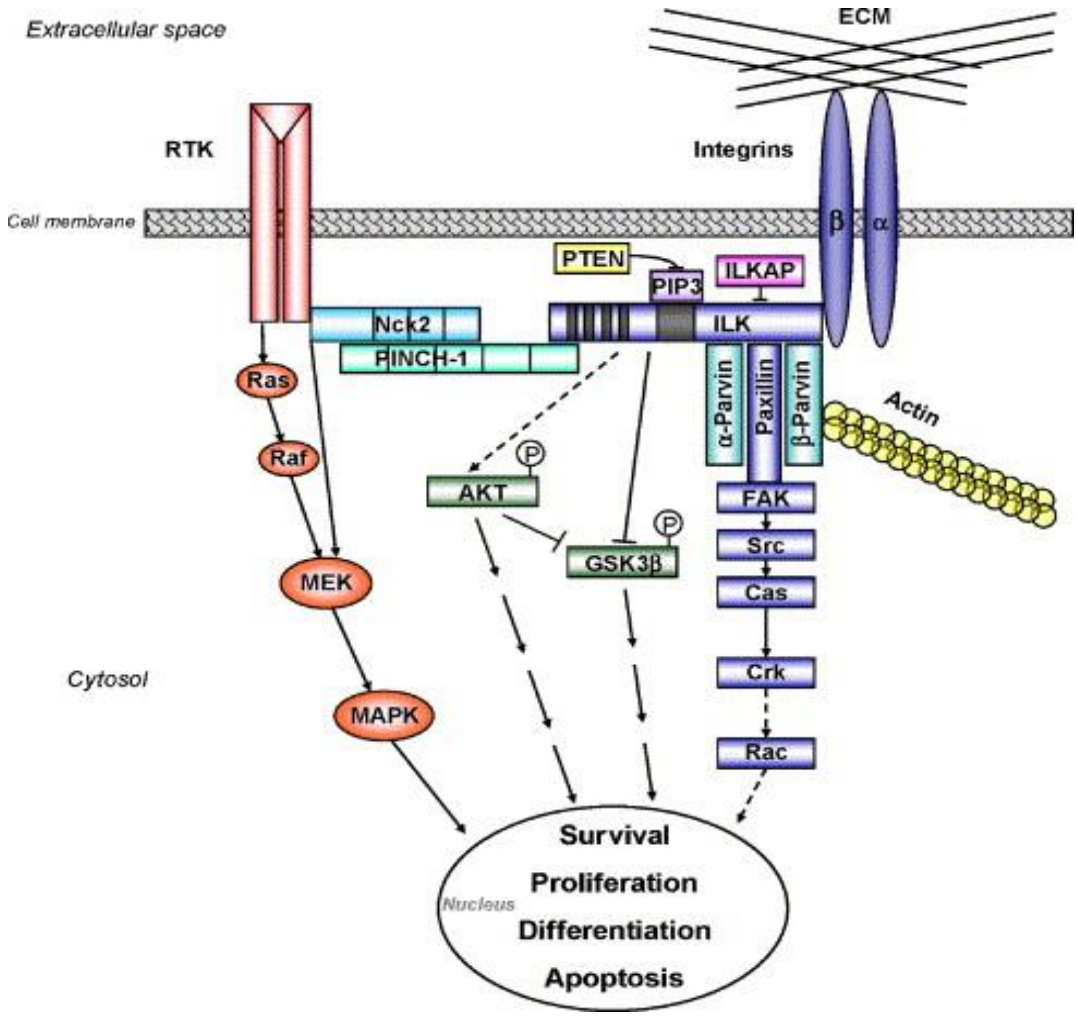

Figure 1.3. Integrin-mediated signalling is facilitated by ILK and FAK.

Integrin receptors lack enzymatic activity, and thereby recruit ILK and FAK to the cytoplasmic side of focal adhesion sites to convey integrin adhesion-based signals at downstream signalling intermediates. ILK and FAK modulate the signalling intermediates in a PI3K-dependent manner, and lead to either their active or inhibitory phosphorylation. ILK and FAK both act as molecular conduits linking adhesion-based signals to downstream signalling intermediates, such as PKB/Akt and GSK3β, thereby facilitating integrin-mediated signalling (Attwell *et al*., 2003).

1.5 Integrin-linked kinase and focal adhesion kinase likely converge adhesion-based survival signals at glycogen synthase kinase 3β

As mentioned, ILK and FAK connect downstream signalling intermediates to integrin signalling pathways through their phosphorylation and subsequent activation or inhibition. Contrary to the activation of PKB/Akt as a result of phosphorylation by ILK and FAK, GSK3β is a 47 kDa Ser/Thr protein kinase that is constitutively active under normal conditions and conversely requires phosphorylation at Ser-9 by interactors such as ILK and FAK to result in inhibition, and phosphorylation at Tyr-216 is required for maximal activity (Cohen and Frame, 2001). The mechanism of regulation of GSK3β is represented in Figure 1.4, below.

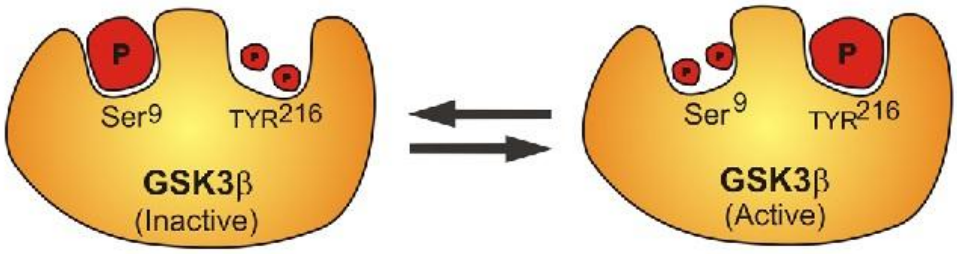

Figure 1.4. Mechanism of the regulation of GSK3β.

Regulation of GSK3β activity occurs primarily as a result of phosphorylation of GSK3β at specific residues by upstream kinases. Phosphorylation of GSK3β at serine 9 results in the N-terminal tail domain of GSK3β to act as a pseudosubstrate by binding to the substrate binding pocket, inhibiting downstream phosphorylation of primed substrates by GSK3β. Conversely, the phosphorylation of GSK3β at tyrosine 216 is required for maximal activity of GSK3β, however; the upstream mechanism resulting in this phosphorylation remains unclear (Seira and del Rio, 2014).

Interestingly, GSK3β has more predicted substrates compared to other kinases, and is therefore suggested to be fundamental to the regulation of almost every process in the cell, however; the interactions between GSK3β and their substrates in these pathways remains to be fully elucidated (Linding *et al*., 2007). As a consequence, dysregulation of GSK3β has been implicated in many pathologies, including diabetes, Alzheimer's disease, Parkinson's disease, and cancer (Jope *et al*., 2007). From this, it is likely that GSK3β is additionally involved in adhesion-based signalling mediated by integrin receptors in epithelial malignancies due to the upstream relationship with ILK and FAK, although the role of GSK3β in integrin-dependent pathways remains poorly understood.

1.6 Glycogen synthase kinase 3β at the intersection of cell death and survival

GSK3β has been shown to elicit contradictory functions depending on the cell type, as well as the signalling environment, further illustrating the complex role of GSK3β in signalling pathways. Specifically with reference to cell survival, GSK3β has exhibited functionality as both a tumour suppressor and tumour promoter according to the cellular context. As such, GSK3β displays the dual capacity to either activate or inhibit apoptosis by regulating a number of downstream survival transcription factors (Beurel and Jope, 2006). The tumour suppressor and pro-apoptotic functionality of GSK3β has been illustrated in cancers such as colorectal cancer and prostate cancer. In these malignancies, as well as in cellular contexts of endoplasmic reticulum (ER) stress and hypoxia, GSK3β has been found to inhibit NF-κB survival signalling, as well as activate p53-induced apoptosis (Cross *et al*., 1995; Kang *et al*., 2010; Yoshino and Ishioka, 2015). In contrast, GSK3β acts as a tumour promoter in cancers such as pancreatic cancer and neuroblastoma by promoting NF-κB survival signalling, inhibiting β-catenin sensitisation to tumour necrosis factor (TNF)-induced cell death, inhibiting activation of apoptosis by c-myc, and inhibiting death-receptor complex formation thereby preventing execution of the extrinsic apoptosis pathway (Kotliarova *et al*., 2008; Sun *et al*., 2008).

Furthermore, the role of inhibited GSK3β in cell death regulation appears contradictory. Suppression of GSK3β activity by phosphorylation at Ser-9 appears to inhibit apoptosis by inhibiting BAX-mediated activation of the mitochondrial apoptosis pathway. Additionally, inhibited GSK3β prevents the inhibition of CREB-dependent expression of anti-apoptotic Bcl-2, resulting in enhanced cell survival (Chuag *et al*., 2011). Consequently, regulation of apoptosis and cell survival by GSK3β in both its active form phosphorylated at Tyr-216 (pGSK3β (Tyr-216)) and inhibited form (pGSK3β (Ser-9)) remain unclear, suggesting that

further research is required to determine the role of GSK3β in the control of survival signalling and apoptosis. Consequently, understanding the role of GSK3β in specific tumour cell types, as well as the integration of ECM-originating signals in GSK3β-mediated survival pathways and apoptosis highlights the therapeutic prospective of targeting GSK3β in epithelial malignancies.

1.7 Regulation of cell survival by the induction of apoptotic events

Programmed cell death by apoptosis occurs as a result of the activation of distinct pathways, intrinsic and extrinsic, that normally functions in modulation of development and homeostasis through eliminating damaged or dysfunctional cells following a cellular stress signal, either intrinsically or extrinsically originating, shown in Figure 1.5. Both intrinsic and extrinsic apoptotic pathways involve a series of events coordinated by signalling intermediates that leads to the activation of zymogenic cysteine proteases called caspases. The activation of specific caspases results in the proteolysis of specific target proteins and subsequently fragmentation of DNA, leading to cell death (Adams and Cory, 2007). Generally, apoptosis serves to maintain the equilibrium between cell survival and cell death, in addition to protecting the integrity of the genome of the cell, functioning as a barrier to malignant transformation (Plati *et al.*, 2008). However, as aforementioned, tumour cells exhibit the aberrant activation of pathways that result in the evasion of cell death, enhancing tumour cell survival. Importantly, the dysfunctional regulation of the initiation apoptotic events not only promotes tumour progression, but also facilitates resistance to therapeutics (Gimenez-Bonafe *et al.*, 2009), emphasising the importance of understanding survival pathways in cancer to improve therapeutic outcomes.

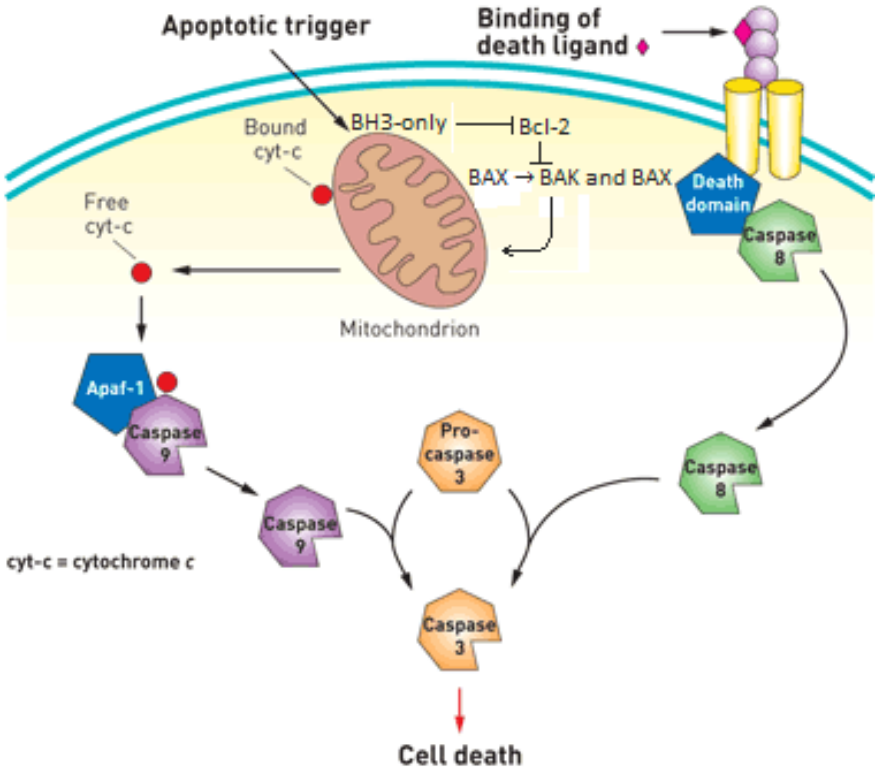

Figure 1.5. The intrinsic and extrinsic pathways of apoptosis executed by caspase 3.

The intrinsic pathway of apoptosis is primarily regulated by the Bcl-2 family of proteins due to their localisation on the mitochondria. During apoptosis, the pro-apoptotic members of the Bcl-2 family trigger cytochrome c release from the mitochondria, ultimately leading to the formation of procaspase 9-activating apoptosome complex. This then results in the activation of caspase 3, and initiation of the execution phase of apoptosis. The extrinsic pathway of apoptosis is activated by binding of extracellular ligands to transmembrane death receptors of the TNF receptor family. Perception of these extracellular ligands results in the recruitment of adaptor proteins, leading to the activation of procaspase 8 and subsequently the execution step of apoptosis initiated by caspase 3 (Guerin *et al*., 2008). (Pro-apoptotic Bcl-2 family members: Bcl-2-associated X protein (BAX), Bcl-2 antagonist/killer (BAK), BH3-only; Anti-apoptotic Bcl-2 family members: Bcl-2)

The Bcl-2 family of proteins are central regulators of the intrinsic pathway of apoptosis, and are central in determining the commitment of a cell to apoptotic cell death or cell survival. The family is composed of two major groups, anti-apoptotic and pro-apoptotic, characterised by their possession of specific Bcl-2 homology (BH) domains (Shamas-Din *et al*., 2013). The anti-apoptotic proteins contain the BH domains 1 to 4, and include Bcl-xL, Bcl-2-related protein A1 (Bfl-1), myeloid cell leukemia protein 1 (Mcl-1), as well as the previously described Bcl-2 (Brunelle and Letai, 2009). The pro-apoptotic proteins contain those with multiple BH domains, such as Bcl-2 homologous antagonist/killer (BAK) and Bcl-2-associated X protein (BAX) or those containing the BH-3 domain only, including Bcl-2-like protein 11 (Bim) and BH-3 interacting-domain death agonist (Bid) (Letai *et al*., 2002).

The importance of the Bcl-2 family of proteins in regulation of cell death is due to their predominant location on the mitochondria, where the release of cytochrome c is controlled. The anti-apoptotic proteins inhibit the pro-apoptotic members, which drive mitochondrial outer membrane permeabilisation (MOMP) and cytochrome c release (Leber *et al*., 2007). The initiation of MOMP by pro-apoptotic Bcl-2 family members and subsequent cytochrome c release, results in the additional release of second mitochondria-derived activator of caspases (SMAC) into the cytoplasm. Cytochrome c then binds to apoptotic protease activating factor 1 (APAF-1), generating the procaspase 9-activating apoptosome complex (Li *et al*., 1997). SMAC then functions in binding and impeding the action of X-linked inhibitor of apoptosis protein (XIAP), an inhibitor of caspase 3, caspase-7 and caspase 9, the effector caspases ultimately responsible for the initiation of the execution step of apoptosis primarily driven by caspase 3 (Schimmer, 2004).

The extrinsic pathway of apoptosis is activated by binding of extracellular ligands to transmembrane death receptors. The death receptors are members of the TNF receptor family which contain a shared cysteine-rich extracellular domain and a cytoplasmic death domain (Locksley *et al*., 2001). The extracellular domain binds ligands, such as first apoptosis signal ligand (FasL) to the Fas receptor (FasR) and TNF-α to TNF receptor 1 (TNFR-1) (Elzey *et al*., 2001). The death domain is then responsible for the transmission of these signals intracellularly, resulting in the recruitment of adaptor proteins, including Fas-associated protein with death domain (FADD). Subsequently, FADD associates with procaspase 8, forming the death-inducing signalling complex (DISC) and results in the activation of caspase 8 (Salvesen and Riedl, 2009). Activation of caspase 8 then results in the induction of the execution step of apoptosis regulated again by the activation of caspase 3, resulting in the

activation of caspase-activated DNase (CAD) leading to DNA fragmentation, as well as cytoskeletal reorganisation and degradation (Sakahira *et al.*, 1998).

1.8 Aberrant regulation of caspase 3 in cancer cell survival and progression

The induction of the execution step of apoptosis which drives cell death is primarily driven by the effector caspase, caspase 3. Therefore, it is unsurprising that aberrant regulation of activity of caspase 3 is a hallmark of cancer cell survival (Hanahan and Weinberg, 2011). Consequently, caspase 3 activity may prove as a useful observational tool in the elucidation of the role of GSK3β in adhesion-mediated survival signalling as an indicator of the induction of cell death by apoptosis. Interestingly, however; in addition to the role of dysfunctional regulation of caspase 3 in the ability to allow cancer cells to evade programmed cell death by apoptosis, caspase 3 has been illustrated to be involved in non-apoptotic pathways also relevant in cell survival. Dysfunctional regulation of caspase 3 has been shown to facilitate chronic inflammation, such as the activation of the pro-inflammatory NF-κB pathway, which drives the production of inflammatory cytokines and chemokines which have been illustrated to increase cancer cell survival (Fernald and Kurokawa, 2013). Further, caspase 3 has been illustrated to regulate cell cycle progression, differentiation, invasion and migration (Frost *et al.*, 2001; Abdul-Ghani and Megeney, 2008; DeNardo et al., 2008). As GSK3β is an upstream regulator of pathways involved in inflammation, proliferation, differentiation, migration and survival, it could be likely that GSK3β additionally regulates caspase 3 activity in epithelial malignancies.

1.9 Human oesophageal squamous cell carcinoma as a highly aggressive malignancy and the molecular events underlying enhanced tumour cell survival

Oesophageal cancer is the eighth most common cancer globally, 95 % of which are of the squamous cell carcinoma histological phenotype. Human oesophageal squamous cell carcinoma (HOSCC) is a highly aggressive cancer of the epithelium lining the upper oesophagus, and is additionally highly invasive with over thirty percent of patients having developed metastases at the time of presentation (Zhang *et al.*, 2013). HOSCC has the widest variation in incidence by geographical location as compared to other carcinoma malignancies, occurring in China, the Middle East, and the Eastern Cape regions of South Africa (Blot and McLaughlin, 1999). As such, HOSCC remains under-investigated due to its prevalence in emerging economy countries despite the aggressive nature of the malignancy. Furthermore, like other gastro-intestinal tract cancers, investigation into the molecular mechanisms

underlying HOSCC has focused predominantly on intrinsic features of the malignancy, as well as the activation of oncogenes (Lin *et al*., 2016).

However, adhesion-based communication between the tumour cell and ECM may also be integral to HOSCC progression and survival. Particularly, environmental triggers can lead to chronic inflammation, resulting in constitutive activation of pro-survival pathways. Overexpression of the survival-relevant NF-κB has also been identified in HOSCC, which may suggest the involvement of GSK3β in survival signalling in HOSCC through upstream perception of environmental constituents (Lin *et al*., 2016). As a result, HOSCC may prove a valuable tool in elucidating the importance of adhesion-dependent signalling and constituents of the ECM and the downstream role of GSK3β in the modulation of survival-relevant pathways, thereby establishing a more comprehensive understanding of the molecular landscape of the malignancy and malignancies which share similar prognostic biomarkers.

CHAPTER 2: Aims and Objectives

2.1 Aim of the Study

The main aim of this research is to investigate the role of glycogen synthase kinase 3β in adhesion-dependent survival signalling and the induction of apoptotic events in human oesophageal squamous cell carcinoma, and the influence of constituents of the extracellular matrix on these pathways.

2.2 Objectives

1. To establish the presence and relative abundance of β1 integrin receptors in HOSCC, and identify the significance of adhesion-dependent interactions mediated by β1 integrin receptors on cell survival by manipulating β1 integrin association with constituents of the extracellular matrix.

2. To determine the relationship between both active and inhibited forms of GSK3β in HOSCC by the detection of pGSK3β (Tyr-216) and pGSK3β (Ser-9), respectively.

3. To manipulate GSK3β signalling in order to identify the role of GSK3β inhibition on cell survival and the induction of apoptosis in HOSCC.

4. To understand the role of the β1 integrin/GSK3β pathway on tumour cell survival via the observation of the induction of the execution step of apoptosis in the form of activated executioner caspase 3.

5. To understand the effects of constituents of the extracellular matrix on GSK3β-mediated adhesion-dependent survival signalling in HOSCC, with specific reference to collagen and fibronectin.

CHAPTER 3: Materials and Methods

3.1 Cell lines

Five oesophageal squamous cell carcinoma cell lines, namely WHCO1, WHCO3, WHCO5, WHCO6 (Veale and Thornley, 1989), and SNO (Bey *et al*., 1976) cell lines derived from moderately differentiated oesophageal tumours of South African origin were obtained from the Cell Biology Research Laboratory stock at the University of the Witwatersrand, Johannesburg. Derived from non-small cell lung cancer (NSCLC) cells of the squamous cell carcinoma histological phenotype, the H1299 cell line was similarly obtained from the Cell Biology Research Laboratory stock and utilised as a positive control cell line, as it is understood that the H1299 cell line is a known expressor of the target protein set. Cell lines derived from oesophageal epithelium considered physiologically normal are unavailable at present (Underwood *et al*., 2010). Oesophageal epithelial cell lines generated as a result of viral transfection exist, however; viral transfection may cause insertional mutagenesis, generating random alterations in gene expression and therefore may have impeded accurate comparison as a consequence of being an untrue representation of normal oesophageal epithelium (Woods *et al*., 2003).

3.2 Tissue culture

The HOSCC and NSCLC cell lines were all maintained on 10 cm plastic tissue culture dishes (NEST, SA) in 3:1 Dulbecco's Modified Eagle's Medium (DMEM)/Ham's F12 Nutrient Mixture (Sigma-Aldrich, USA) (Appendix A, Section 1.3), growth medium supplemented with 10% foetal calf serum (FCS) (Highveld Biological, SA). The cells were maintained under standard conditions at 37ºC in a humidified incubator with 5% carbon dioxide as to facilitate the bicarbonate buffer system employed to buffer the pH of the tissue culture medium. To maintain the health and molecular integrity of the cells, the cells were passaged and sub-cultured when grown up to approximately 75% confluency on the 10 cm plastic tissue culture dishes. In order to passage the cells, the medium was aspirated and the cells were washed with 2 mL phosphate-buffered saline (PBS) (Appendix A, Section 1.1). Cells are grown to 75% confluency to ensure that the cells are actively replicating and viable, as well as to prevent the induction of contact inhibition of cell growth.

Thereafter, the cells were treated with 2 mL trypsin/ethylenediaminetetra-acetic acid (EDTA) (TE) (Sigma-Aldrich, USA) (Appendix A, Section 1.2) solution and incubated at 37ºC for 5 minutes to detach the cells from the tissue culture dish. A small volume of trypsinised cells

was resuspended in 10 mL fresh growth medium and maintained at standard temperature, humidity, and carbon dioxide levels until required or until further passaging was necessary.

Cells were harvested at approximately 75% confluency for all experimentation conducted.

3.3 Effect of extracellular matrix composition on HOSCC behaviour

3.3.1 Growth of cells on collagen type I-coated substrate

A collagen type I working solution with a final concentration of 100 µg/mL was prepared from a 3 mg/mL collagen type I stock solution extracted from rat-tail tendon (Appendix A, Section 2.1). To each 6 cm plastic tissue culture dish, 600 µL of collagen type I working solution was added. The solution was swirled to ensure the dish was fully coated. The coated dishes were subsequently exposed to ultraviolet (UV) light for 2.5 hours without the lid to allow the collagen type I solution polymerise completely. Once dried, the coated dishes were washed with sterilised, deionised water three times to remove residual acetic acid. Thereafter, the dishes were washed once with PBS.

Cells were seeded as normal at a density of 8×10^5 cells per 6 cm dish, and maintained under standard conditions for 24 hours, prior to experimentation.

3.3.2 Growth of cells on fibronectin-coated substrate

Using a 1 mg/mL fibronectin stock solution (Roche, Switzerland), a fibronectin working solution at a final concentration of 10 µg/mL was prepared (Appendix A, Section 2.2). To each 6 cm plastic tissue culture dish, 1 mL of the fibronectin working solution was added, and swirled to ensure the bottom of the dish was completely coated. The dishes were then exposed to UV light for 45 minutes with the lid on to allow the fibronectin solution to polymerise. Following this, the remaining fibronectin solution was removed from the dishes, and the cells were seeded immediately as normal at a density of 8×10^5 cells per 6 cm dish.

Cells were maintained under standard conditions for 24 hours prior to experimentation.

3.4 Role of GSK3β regulation in HOSCC cell survival

3.4.1 Targeted inhibition of GSK3β

From a 5 µg/µL stock solution of AR-A014418, a GSK3β-specific inhibitor, a working solution of 10 µM dissolved in DMSO was introduced to each 6 cm tissue culture dish with cells grown to approximately 75% confluency with DMSO-only controls additionally plated for each cell line. Cells were maintained under standard conditions for 24 hours prior to

experimentation, however; cells were grown for 1 hour in the presence of the GSK3β inhibitor prior to whole-cell protein extraction for western immunoblotting.

3.5 Whole-cell protein extraction

Double Laemmli lysis buffer (Laemmli, 1970) was utilised in the whole-cell protein extraction protocol due to the localisation of GSK3β and caspase 3 in the cytoplasm, as well as the transmembrane localisation of β1 integrin at the cell-ECM interface. A whole-cell protein extraction was performed considering immunodetection of the target protein set was performed in subsequent experimentation. Cells grown to 75% confluency were washed twice with 2 mL ice-cold PBS. Thereafter, 1 mL 1:100 phenylmethylsulphonyl fluoride (PMSF) (Sigma-Aldrich, USA) (Appendix A, Section 3.1)/PBS solution was added to each dish. Cells were harvested using a sterilised cell scraper into the PMSF/PBS solution. The harvested cell suspension was aspirated into sterile microcentrifuge tubes and centrifuged in a TOMY desktop centrifuge at 13 817 RCF for 2 minutes. The supernatant was discarded and the pellet resuspended in double Laemmli lysis buffer (Appendix A, Section 3.2). The resuspended samples were incubated at 100ºC in a boiling water bath for 5 minutes. Subsequently, the samples were centrifuged at 4ºC in a PRISM™ Refrigerated Microcentrifuge for 15 minutes at 12 000 RCF.

All whole-cell extracts were stored at -20ºC.

3.6 Quantitative determination of protein concentration

Estimation of protein concentration was performed according to a modified protocol established by Bramhall *et al*. (1969). The Bramhall method of protein estimation was performed as alternative protocols such as the Bradford assay are incompatible with SDS-containing samples. This protocol has been optimised for whole-cell lysates that have been extracted using lysis buffers containing sodium dodecyl sulphate (SDS), such as double Laemmli lysis buffer.

Circular Whatman® filter paper was washed in deionised water for 20 minutes prior to dehydration in 95% ethanol, 100% ethanol and 100% acetone for 5 minutes each, respectively. Following dehydration, the filter paper was air-dried under a fume hood for approximately 10 minutes. Using a 1 mg/mL bovine serum albumin (BSA) stock solution diluted in double Laemmli lysis buffer (Appendix A, Section 3.3), standard concentrations of the BSA solution (1 µg/µL, 3 µg/µL, 6 µg/µL, 12 µg/µL, 16 µg/µL and 20 µg/µL) were spotted onto the filter paper to construct a standard curve. Similarly, 2 µL of extracted protein

sample were spotted onto the filter paper. The filter paper was left to air-dry for approximately 15 minutes and subsequently fixed with 7.5% trichloroacetic acid (TCA) (Appendix A, Section 3.4) for 45 minutes. Following incubation in TCA, Coomassie Brilliant Blue stain (Appendix A, Section 3.5) was added and the filter paper incubated in the stain wash for 5 minutes. Thereafter, the stain was discarded and fresh Coomassie Brilliant Blue stain added to the filter paper and incubated for 1 hour on an orbital shaker, after which the filter paper was incubated in destain solution (Appendix A, Section 3.6) for 1 hour. The destained filter paper was air-dried under a fume hood and the stained circles of spotted BSA standard or sample were cut out, placed into test tubes containing 5 mL elution solution (Appendix A, Section 3.7) and incubated overnight in the dark.

The absorbencies of the eluted protein solutions were determined at 595 nm using an Azzota SV1100 Spectrophotometer.

3.7 Sodium dodecyl sulphate-polyacrylamide gel electrophoresis (SDS-PAGE)

Discontinuous SDS-PAGE was performed as per the protocol established by Laemmli (1970).

The polyacrylamide gels were composed of a stacking gel and a separating gel of varying amounts of acrylamide. For separation of the whole cell lysates for subsequent immunodetection of the target protein set, a 10% (w/v) separating gel was utilised for the separation of the whole cell lysates into the respective molecular weight ranges containing β1 integrin, pGSK3β (Tyr-216), pGSK3β (Ser-9) and caspase 3 polypeptides. For all SDS-PAGE, a 5% stacking gel was used. Gels were constructed in the Mighty Small™ SE245 Dual Gel Caster apparatus (Hoefer Scientific, USA). The separating polyacrylamide gel solution (Appendix A, Section 4.2) was first poured into the casting apparatus between the glass and silicon plates sterilised with isopropanol before use. Thereafter, 200 µL 4% sodium dodecyl sulphate (SDS) overlay solution (Appendix A, Section 4.4) was added to facilitate polymerisation. The separating gel was allowed to polymerise for approximately 30 minutes. The SDS overlay solution was subsequently removed and the stacking gel solution (Appendix A, Section 4.3) was poured over the separating gel, immediately followed by insertion of a 10-well comb. The stacking gel was allowed to polymerise for approximately 15 minutes. The polymerised gels were placed in the Mighty Small II SE 250 Mini Vertical Electrophoresis Unit (Hoefer Scientific, USA) and the apparatus filled with SDS-PAGE running buffer (Appendix A, Section 4.5). Thereafter, an equal 30 µg of each protein sample

was loaded into the respective wells in volumes determined by protein estimation (Section 3.6). PageRuler™ Plus Prestained Protein Ladder (ThermoScientific, USA) was loaded to track progression of electrophoresis and to identify the molecular weight corresponding to the separated proteins in the target set. The proteins were separated on the gel at a constant 21 mA/gel for 45 minutes.

3.8 Antibodies for immunodetection during Western immunoblotting

Immunological analysis employing an indirect antibody detection system was employed during western immunoblotting to detect specific epitope sites on the target proteins, forming an immunogen complex. Primary antibodies specific to each of the target proteins were utilised. Polyclonal antibodies were used as the antibodies bind more epitope sites on the specific target protein than monoclonal antibodies, thereby amplifying the detection signal. For the detection of β1 integrin, a mouse polyclonal anti-β1 integrin primary antibody (Merck, SA) at a concentration of 1:10 000 was used in a diluent of 2.5% non-fat dried milk powder in tris-buffered saline with 0.1% Tween 20 (TBS-T). The immunodetection of pGSK3β (Tyr-216) was performed using a rabbit polyclonal anti-pGSK3β (Tyr-216) primary antibody (Abcam, UK) at a concentration of 1:2 000 diluted in 2.5% BSA TBS-T. The primary antibody used for the detection of the 47 kDa pGSK3β (Tyr-216) polypeptide additionally confers the detection of the 51 kDa pGSK3α (Tyr-279). For the detection of pGSK3β (Ser-9) a rabbit polyclonal anti-pGSK3β (Ser-9) primary antibody (Cell Signaling Technology, USA) was used at a concentration of 1:1 000 diluted in 2.5% BSA TBS-T. A rabbit polyconal anti-caspase 3 primary antibody (Santa Cruz Biotechnology, USA) at a concentration of 1:500 in a diluent of PBS was used for specifically detecting cleaved, activated caspase 3. The detection of β-actin was performed using rabbit polyclonal primary antibodies (Cell Signaling Technology, USA) at a concentration of 1:2 500 2.5% milk in PBS. β-actin was used as the loading control for all western immunoblotting experiments conducted to ensure equal loading of sample into each well and to validate that differential expression levels are a result of changes in cellular behaviour and not due to experimental variances.

For the detection of bound primary antibody to β1 integrin by chemiluminescence, a goat anti-mouse horseradish peroxidase (HRP)-conjugated secondary antibody was used (Cell Signaling Technology, USA). The chemiluminescent detection and visualisation of pGSK3β (Tyr-216), pGSK3β (Ser-9), and cleaved caspase 3 was performed using the same goat anti-rabbit HRP-conjugated secondary antibody (Separations Scientific, SA).

3.9 Western immunoblotting

Western immunoblotting was performed according to the protocol described by Towbin *et al.* (1979).

Approximately 30 µg of each whole-cell extract was separated on a 10% (w/v) polyacrylamide gel, and the sections of the gel presumed to contain the proteins of interest based on the positioning of the PageRuler™ Plus Prestained Protein Ladder were excised. The gel sections were placed on sponges pre-soaked in transfer buffer (Appendix A, Section 5.3), and accordingly Hybond C nitrocellulose membranes (Sigma-Aldrich, USA) were cut to size and placed over the gel sections. The excised gel sections containing the proteins of interest were transferred using a BioRad Criterion™ wet transfer blotting apparatus (BioRad, USA) for 1 hour for caspase 3, and 2 hours for β1 integrin, pGSK3β (Tyr-216), pGSK3β (Ser-9) and β-actin at a constant current of 400 mA at 4ºC.

Post-transfer, the nitrocellulose membranes were washed for 5 minutes in TBS (Appendix A, Section 5.1) and thereafter incubated for 1 hour in blocking buffer solution (Appendix A, Section 5.4). The membranes were subjected to three 5 minute washes in TBS-T (Appendix A, Section 5.2), and incubated in primary antibody overnight at 4ºC. Following incubation in primary antibody, the membranes were washed three times for 5 minutes each with TBS-T and then incubated in HRP-conjugated secondary antibody for 1 hour in the dark at room temperature (β1 integrin, pGSK3β (Tyr-216), pGSK3β (Ser-9) and caspase 3) or at 30ºC (β-actin). Subsequent to incubation in secondary antibody, the membranes were washed three times for 5 minutes each with TBS-T and once for 5 minutes in TBS in the dark. To catalyse the chemiluminescent reaction, 820 µL of both SuperSignal® West Pico luminol and peroxide (ThermoFisher, USA) was added to each membrane and incubated for 2 minutes in the dark. Following incubation in chemiluminescent substrate, excess luminol and peroxide solution was blotted off of the membranes using paper towel and sealed in plastic wrap. The membranes were placed in an x-ray film cassette and exposed to clear-blue CL-XPosure™ x-ray film (Pierce Biotechnology, USA) in a darkroom for 10 minutes. Immediately following exposure, the x-ray film was briefly incubated in developing solution (Appendix A, Section 5.5) for approximately 10 to 20 seconds, subsequently washed in water, placed in fixing solution (Appendix A, Section 5.6) until clear, followed by a final rinse in water.

3.10 Densitometric analysis

Densitometric analysis was performed on the western immunoblots in order to quantitatively ascertain the expression levels of the proteins of interest. Densitometry facilitates semi-quantitative determination of protein expression as a result of comparison between the optical densities of the reference band and those produced by the HOSCC samples. Furthermore, considering the narrow linear range exhibited by x-ray film, densitometry software regularises background on scanned images, providing a means for comparison. Densitometry was performed using ImageJ (Schneider *et al*., 2012).

3.11 MTT cell proliferation assay

In order to evaluate the effect of altered ECM, as well as the role of GSK3β on the proliferative activity of HOSCC and subsequently cell survival, an MTT assay was performed according to the protocol developed by Mosmann (1983).

To cells grown to approximately 75% confluency, tissue culture medium was aspirated off of the cells and then washed twice with sterile PBS. Subsequently, fresh tissue culture medium containing 0.25 mg/mL of the 3-(4,5-dimethylthiazol-2-yl)-2,5-diphenyltetrazolium bromide (MTT) tetrazolium dye (Appendix A, Section 6.1) was added to each tissue culture dish. The cells were then incubated for 2 hours in the dark in a humidified incubator at 37ºC. Following incubation, 1 mL isoproponal was added to solubilise the insoluble purple formazan crystals, the by-product of the reduction of the MTT dye by mitochondrial succinate dehydrogenase of actively respiring and proliferating cells, and incubated for 1 hour in the dark on an orbital shaker.

Absorbencies were read at 570 nm using an Azzota SV1100 Spectrophotometer.

3.12 Crystal Violet cell adhesion assay

Observation of alterations in cell adhesion was performed using a Crystal Violet cell adhesion assay following a modified protocol established by Humphries (2009).

Cells were seeded at a density of 3×10^5 cells in each 3.5 cm tissue culture dish for each experimental condition and incubated at 37ºC for 24 hours. The medium was aspirated off of the cells. Following this, cells were washed twice with sterile PBS, and 2 mL 0.5% Crystal Violet staining solution (Appendix A, Section 7.1) was added to each tissue culture dish. The cells were incubated for 20 minutes at room temperature on an orbital shaker in the dark. Subsequently, the tissue culture dishes were washed gently using a Pasteur pipette and

distilled water to remove excess Crystal Violet stain. Excess water was removed by tapping the tissue culture dishes on paper towel, and the tissue culture dishes were allowed to dry overnight. Once dried, 5 mL methanol was added to each dish, and the dishes were incubated for 20 minutes at room temperature on an orbital shaker in the dark.

The absorbencies of each sample were read at 570 nm using an Azzota SV1100 Spectrophotometer.

3.13 Trypan Blue quantitation of cell death

Quantitation of cell death using Trypan Blue was performed as per a modified protocol established by Uliasz and Hewett (2000).

Cells were seeded at a density of 3×10^5 cells per 3.5 cm tissue culture dish for each experimental condition and incubated at 37ºC for 24 hours until grown to 75 % confluency. 600 µL of 0.4% Trypan Blue solution (Appendix A, Section 8.1) was added to each dish, except the blank, and incubated for 15 minutes at 37ºC in a humidified incubator. The assay is performed under the principle that live cells exclude the Trypan Blue dye, whereas dead, non-viable cells exhibit compromised cell membranes and will absorb the dye. The medium containing the Trypan Blue solution was subsequently removed through gentle washing using ice-cold and sterile PBS as to not agitate any dead cells in the tissue culture dishes. Following washing, 1.5 mL 1% (w/v) SDS solution (Appendix A, Section 8.2) was added to each dish to release the dye into solution.

The absorbencies of each sample were measured at 590 nm using an Azzota SV1100 Spectrophotometer.

3.14 Statistical evaluation

Where applicable, a Student's t-test was performed in order to determine whether the relative expression levels observed were statistically significant between samples, and differences in expression levels and sample means were not a result of experimental error. Results with statistical significance ($p < 0.05$) will be indicated with an asterisk (*). Error bars on resultant plots are representative of standard error of the mean (SEM). Additionally, percentage change was calculated as follows:

$$\%\, change = \frac{(treated - untreated)}{untreated}$$

CHAPTER 4: Results

4.1 HOSCC cells exhibit a differential abundance of both active and inactive phosphorylated forms of GSK3β

The mechanism of regulation of GSK3β appears complex, such that the enzyme is constitutively active under normal conditions and the phosphorylation at Ser-9 by interactors such as ILK and FAK results in the inhibition and inactivation of GSK3β, and phosphorylation at Tyr-216 is required for maximal activity. From this, it is likely that GSK3β is involved in adhesion-based signalling mediated by integrin receptors in epithelial malignancies due to the upstream relationship with ILK and FAK, although the role of GSK3β in integrin-dependent pathways remains poorly understood.

Furthermore, both phosphoylated forms of GSK3β have been shown to elicit contradictory functions depending on the cell type, as well as the signalling environment, specifically with reference to cell survival. To first evaluate the relative abundance and therefore the relationship between both phosphorylated forms of GSK3β in adhesion-based cell survival in HOSCC under standard conditions, western immunoblotting and densitometric analyses were performed. Following western immunoblotting illustrated in Figure 4.1.1, it was revealed that both the inactive (pGSK3β (Ser-9)) and active (pGSK3β (Tyr-216)) phosphorylated forms of GSK3β are present in each of the HOSCC cell lines as determined by the immunodetection of the respective 47 kDa polypeptide. Additionally present in the immunoblots for the detection of pGSK3β (Tyr-216) is the 51 kDa polypeptide indicative of pGSK3α (Tyr-279). Further, densitometric evaluation showed that each HOSCC cell line exhibits varying abundance of each of the phospho-forms of GSK3β, as seen in Figure 4.1.2.

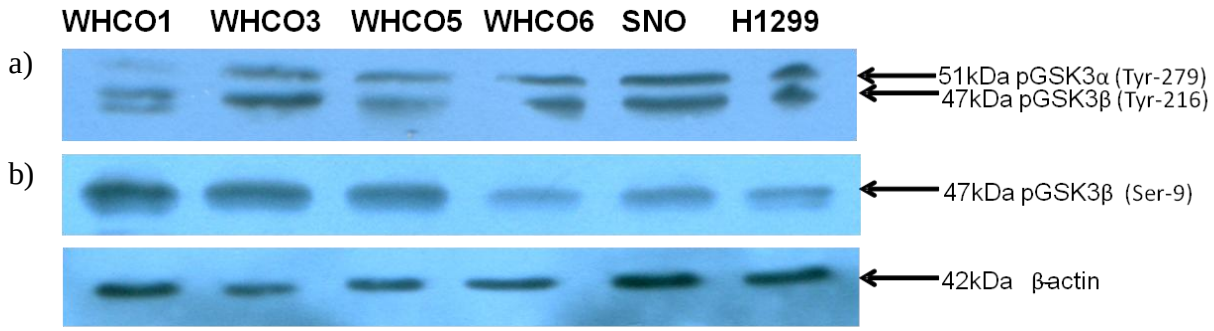

Figure 4.1.1. Both active and inactive phosphorylated forms of GSK3β were detected in HOSCC cells.

The whole-cell protein extracts were resolved on a 10% (w/v) SDS-PAGE gel and subject to western immunoblotting analyses. Western immunoblotting determined the presence of a) pGSK3β (Tyr-216) and b) pGSK3β (Ser-9) in all HOSCC cell lines conferring a respective molecular weight of 47 kDa, and at elevated levels with respect to the control, as well as the 51 kDa pGSK3α (Tyr-279). The H1299 NSCLC cell line was used as a comparative control, known to exhibit elevated levels of both active and inactive phosphorylated forms of GSK3β. Moreover, each HOSCC cell line appeared to exhibit varying levels of both pGSK3β (Tyr-216) and pGSK3β (Ser-9). β-actin was used as a loading control in order to ensure equal loading of each protein sample. Note: The immunoblots shown are representative of three independent experiments (n = 3).

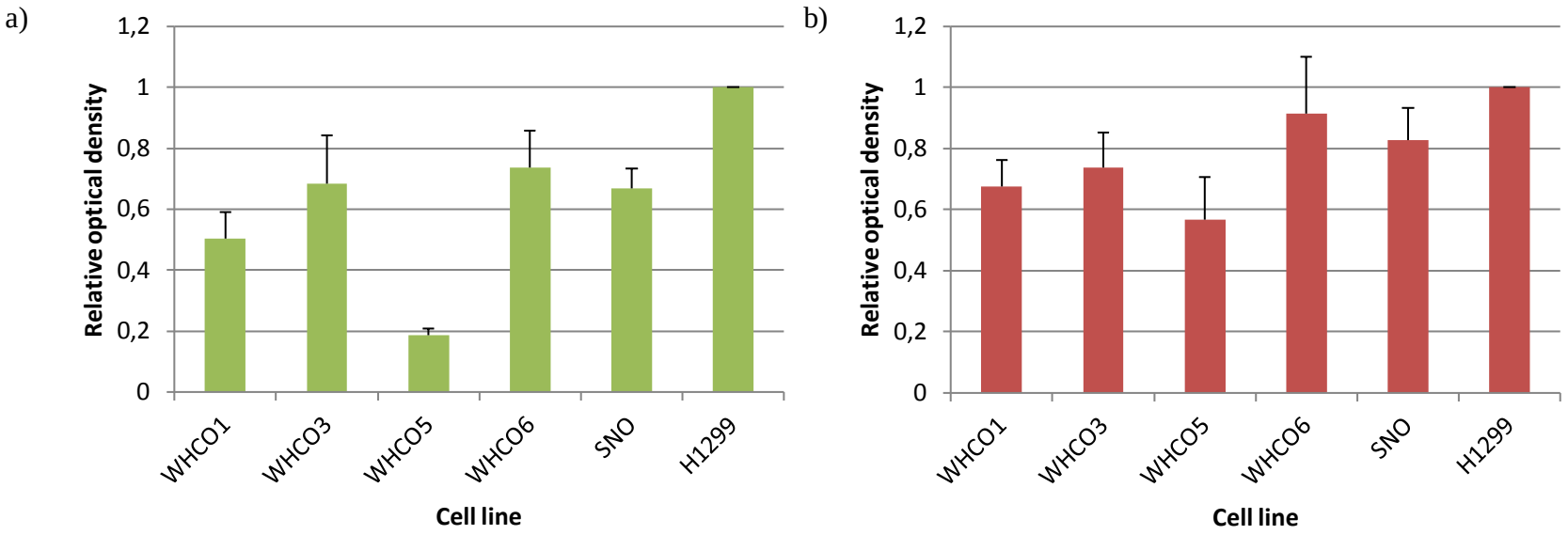

Figure 4.1.2. HOSCC cells exhibit a varying and elevated abundance of both phosphorylated forms of GSK3β.

Following western immunoblotting analyses, the resultant immunoblots were subject to densitometric evaluation using ImageJ to allow for the semi-qualitative determination of variances in abundance of a) pGSK3β (Tyr-216) and b) pGSK3β (Ser-9). The H1299 NSCLC cell line was used as a comparative control due to its known over-expression of both phospho-forms of GSK3β. From the densitometric analyses, it can be seen that the HOSCC cell lines exhibit relatively high levels of both the phosphorylated forms of GSK3β, with the exception of the WHCO5 cell line, revealing a significantly lower abundance of the active pGSK3β (Tyr-216) in comparison to each cell line. Note: The densitometry shown is a result of three independent experiments (n = 3).

The H1299 NSCLC cell line is a known overexpressor of GSK3β (Zeng *et al*., 2014), and was therefore used to comparatively analyse the abundance of both phosphorylated forms of GSK3β in HOSCC cells. As a result, it can be seen in Figure 4.1.2 that the inactive (pGSK3β (Ser-9)) and active (pGSK3β (Tyr-216)) phospho-forms are present in varying, yet elevated levels in HOSCC cells when compared to the H1299 control cell line under standard tissue culture conditions. Exhibiting the highest abundance of pGSK3β (Ser-9) in the HOSCC cell lines is the WHCO6 cell line, with a marginal 8% difference between the abundance of the inactive form of GSK3β (pGSK3β (Ser-9)) in the H1299 cell line. The WHCO1, WHCO3 and SNO cell lines were similarly revealed to exhibit high levels of inactive GSK3β. In contrast, the lowest abundance of inactive GSK3β was observed in the WHCO5 cell line, with a 43% lower abundance than the H1299 control cell line.

Again, varying levels of active GSK3β (pGSK3β (Tyr-216)) were detected in each of the moderately differentiated HOSCC cell lines following Western immunoblotting and densitometric evaluation. Surprisingly, it was found that the general levels of active GSK3β were similar to those of inactive GSK3β in HOSCC cells, with no discernible prevalence of either phospho-form. As with the levels of inactive GSK3β observed, it was found that the most elevated abundance of active GSK3β was observed in the WHCO6 cell line in comparison to the H1299 control cell line, followed by the WHCO3 cell line and the SNO cell line. In contrast, the WHCO1 cell line exhibited a low abundance of active GSK3β, however; the WHCO5 cell line exhibited a significantly lower abundance of active GSK3β (pGSK3β (Tyr-216)), with a 32% difference in abundance in comparison to the WHCO1 cell line, and a significant 81% lower abundance than the H1299 control cell line.

4.2 HOSCC cells exhibit varying yet elevated levels of β1 integrin receptors

Aberrant communication between cells and ECM as facilitated by integrin receptors has been shown to modulate tumour cell survival through the dysfunction of downstream signalling pathways. Specifically in epithelia, dysfunctional adhesion signalling mediated by β1 integrin receptors may be a fundamental mechanism in the development and maintenance of HOSCC. In order to determine the significance of adhesion-dependent interactions between β1 integrin receptors in GSK3β-mediated, survival-relevant signalling in HOSCC, the presence and relative abundance of β1 integrin receptors was established through western immunoblotting and densitometric evaluation, shown in Figure 4.2, and revealed elevated, yet varying levels of β1 integrin receptors in HOSCC.

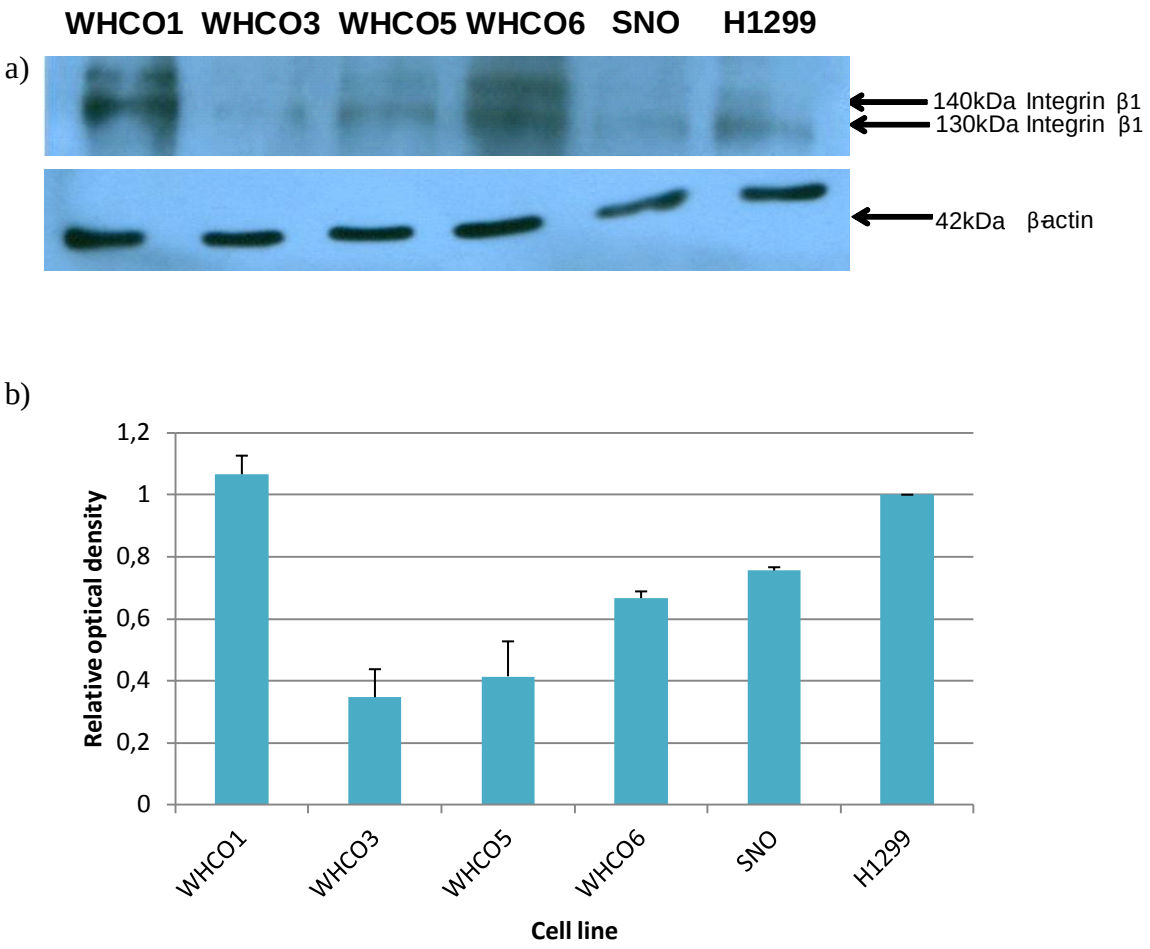

Figure 4.2. β1 integrin receptors are present at varying abundance levels in HOSCC cells.

a) Western immunoblotting performed on whole-cell protein extracts resolved on a 10% (w/v) SDS-PAGE gel indicated the presence of β1 integrin receptors in all HOSCC cell lines conferring a molecular weight of 130 kDa. Additionally, each of the HOSCC cell lines was found to express a polypeptide of a higher molecular weight, conferring a molecular weight of 140 kDa. The H1299 NSCLC cell line was used as a comparative control due to its known elevated abundance of β1 integrin receptors. β-actin was used as a loading control to ensure equivalent loading. b) Subsequent densitometric analyses were performed on the 130 kDa polypeptide bands observed on the resultant immunoblots using ImageJ indicated that each HOSCC cell line exhibit a varying abundance of β1 integrin receptors. Note: The immunoblots and densitometry shown are representative of three independent experiments (n = 3).

The presence of β1 integrin receptors was determined in all of the HOSCC cell lines following western immunoblotting as indicated by the immunodetection of the 130 kDa polypeptide, shown in Figure 4.2a. Furthermore, densitometric evaluation revealed differential levels of abundance of β1 integrin receptors in all HOSCC cell lines, as indicated in Figure 4.2b. The most elevated level of β1 integrin receptors was observed in the WHCO1 cell line, followed by the H1299 NSCLC control cell line. The SNO and WHCO6 cell lines similarly revealed a high abundance of β1 integrin receptors. The lowest levels of β1 integrin receptors was observed in the WHCO3 cell line, followed by the WHCO5 cell line with a minimal (< 1%) difference between the levels of β1 integrin. In addition to the immunodetection of the 130 kDa β1 integrin polypeptide, a 140 kDa isoform of β1 integrin was present in all five HOSCC cell lines.

Interestingly, it was observed that in the WHCO1, WHCO6 and SNO cell lines, an elevated abundance of the inactive phospho-form of GSK3β (pGSK3β (Ser-9)) corresponded with elevated levels of β1 integrin receptors. In the WHCO6 and SNO cell lines, it was found that an elevated abundance of β1 integrin receptors corresponded with a high abundance of active GSK3β (pGSK3β (Tyr-216)). In contrast, the WHCO3 cell line displayed a low abundance of β1 integrin receptors, yet a high abundance of both phosphorylated forms of GSK3β. This similar trend in the correspondence between levels of both active and inactive GSK3β and β1 integrin receptors may suggest concomitant regulation of GSK3β by β1 integrin-mediated pathways. In the WHCO5 cell line, it was observed that a lower abundance of β1 integrin receptors corresponded with low levels of both phosphorylated forms of GSK3β. In general, it is therefore apparent that higher levels of β1 integrin correspond with a more elevated abundance of inactive GSK3β. Considering β1 integrin-mediated signalling is facilitated primarily through interactors associated with downstream inhibitory phosphorylation of GSK3β, it is likely that the inactive phospho-form of GSK3β may be a more significant interactor in β1 integrin-mediated signalling in HOSCC cells than the active phosphorylated form of GSK3β.

4.3 β1 integrin receptors may facilitate the adhesion of HOSCC cells

β1 integrin receptors are the most widely expressed integrin receptor in epithelial tissue. Consequently, β1 integrin receptors remain indispensible to appropriate ligation and communication between epithelial cells and constituents of the ECM. Further, in solid tumour malignancies, it has been shown that aberrant expression of β1 integrin receptors contributes

to the development and progression of the malignancy. In order to identify the significance of β1 integrin receptors in the adhesive properties of HOSCC cells, as well as the relationship between adhesion and survival signalling, a Crystal Violet cell adhesion assay was performed on the HOSCC cells, shown in Figure 4.3, and displayed elevated levels of cell adhesion.

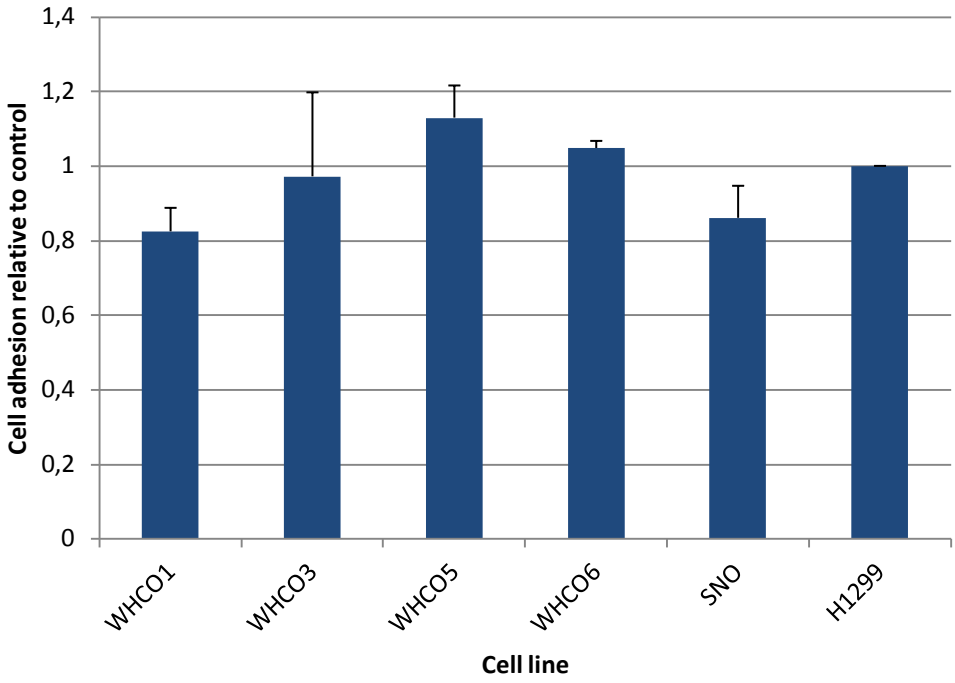

Figure 4.3. HOSCC cells show variable yet high levels of cellular adhesion.

Crystal Violet qualitative cell adhesion evaluation was performed on each moderately differentiated HOSCC cell line with cells seeded at 3×10^5 cells in each 3.5 cm tissue culture dish after 24 hours under standard conditions, and absorbencies measured at 570 nm. It was revealed that each HOSCC cell line exhibited varying levels of cell adhesion with respect to the H1299 NSCLC cell line used as a comparative control. Note: The results shown are representative of three independent experiments (n = 3).

Following growth of each HOSCC cell line for 24 hours under standard conditions, it was found that each HOSCC cell line exhibited high adhesion to the tissue culture dish when compared to the H1299 control cell line, as seen in Figure 4.3. However, each of the HOSCC cell lines displayed variable adhesion. It was observed that the WHCO5 had the highest level of adhesion with a 13% more elevated level of adhesion in comparison to the H1299 control cell line, followed by the WHCO6 and WHCO3 cell lines. The lowest adhesion was seen in the WHCO1 cell line, with a 18% lower level of adhesion than the H1299 control cell line. Interestingly, the level of cell adhesion was found not to correspond proportionally with the abundance of β1 integrin receptors illustrated in Figure 4.2. This may be suggestive that adhesion of HOSCC cells to a substrate is facilitated by a mechanism other than, or in conjunction with, β1 integrin receptors.

4.4 HOSCC cells display varying abundance of activated caspase 3

Normally, the induction and execution of programmed cell death in the form of apoptosis occurs as a natural barrier to cancer development via the elimination of cells exhibiting dysfunctional cell signalling and behaviour. Following the perception of a cellular stress signal, apoptotic signalling is initiated and executed following the proteolytic cleavage of the 32 kDa zymogenic cysteine protease caspase 3 at Asp-175 and into its activated subunits conferring molecular weights of 12 kDa and 17 kDa, respectively.

However, tumour cells exhibit aberrant apoptotic signalling, favouring pro-survival pathways and selective growth advantages that hinder the induction of apoptosis by blocking the execution step carried out by activated caspase 3 through mechanisms such as over-expression of XIAP (Schimmer *et al.*, 2006). In order to analyse the role of the β1 integrin/GSK3β pathway in survival signalling, analysis of the downstream cleavage and activation of caspase 3 was performed by immunodetection and densitometric evaluation, shown in Figure 4.4, and revealed the detection of activated caspase 3 in all HOSCC cell lines at varying levels of abundance.

a)

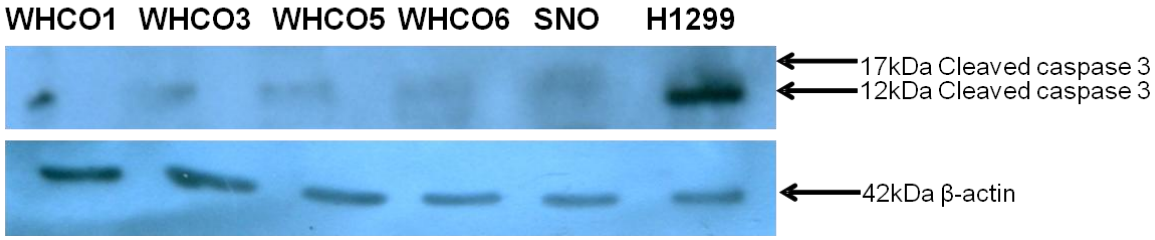

b)

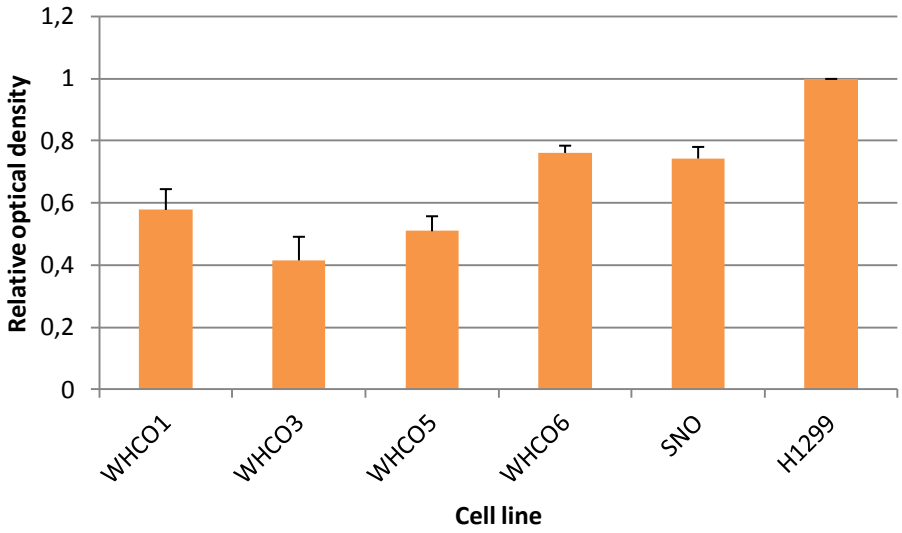

Figure 4.4. Activated caspase 3 is present at relatively low levels in HOSCC cells.

a) Western immunoblotting performed on whole-cell protein extracts resolved on a 10% (w/v) SDS-PAGE gel indicated the presence of the activated form of caspase 3 through the detection of the cleaved products of pro-caspase 3, conferring molecular weights of 12 kDa and 17 kDa. b) Densitometric evaluation performed on the 12 kDa polypeptide bands on the resultant immunoblots using ImageJ revealed varying levels of cleaved and therefore activated caspase 3 in all HOSCC cell lines using the H1299 cell line as a comparative control. Note: Densitometry shown is representative of three experiments (n = 3).

From western immunoblotting and subsequent densitometric analyses, it was observed that the HOSCC cells exhibited differential abundance of activated caspase 3, as indicated through immunodetection of the 12 kDa and 17 kDa cleaved products of pro-caspase 3. It is apparent that the HOSCC cells have a lower overall abundance of activated caspase 3 in comparison to the H1299 control cell line, indicative of less induction of apoptotic events in the HOSCC cell lines. The highest abundance of activated caspase 3 was observed in the H1299 control cell line, followed then by the WHCO6 cell line, with a 7% lower abundance than the H1299 control cell line, followed then by the SNO cell line. The lowest level of activated caspase 3 was identified in the WHCO3 cell line, with a 45% lower abundance than the H1299 control cell line. In the WHCO1, WHCO6 and SNO cell lines, the relatively elevated level of activated caspase 3 corresponds with elevated levels of both β1 integrin receptors and inactive GSK3β (pGSK3β (Ser-9)). Conversely, a lower abundance of β1 integrin receptors observed in the WHCO3 and WHCO5 cell lines corresponded with a low level of activated caspase 3. This may suggest that the HOSCC cells may be dependent on appropriate adhesive cues transmitted by β1 integrin receptors and regulated by GSK3β for survival advantages and the hindrance of the induction of apoptotic events.

4.5 β1 integrin receptors and GSK3β appears to modulate tumour cell proliferation and tumour cell death in HOSCC

In order to sustain the increased energy demand to facilitate proliferative advantages which allow malignancies to develop and progress, dysfunction of metabolic signalling often occurs (Luengo *et al*., 2017). This selective growth advantage contributes to cancer cell survival, proliferation and migration, thus the observation of the metabolic and proliferative behaviour in malignancies will provide further insight into the role of β1 integrin/GSK3β pathways in HOSCC cell survival.

It was revealed that HOSCC cells exhibited elevated levels of cellular proliferation under standard, non-stimulated conditions, seen in Figure 4.5.1, following MTT cell proliferation assays conducted under standard tissue culture conditions.

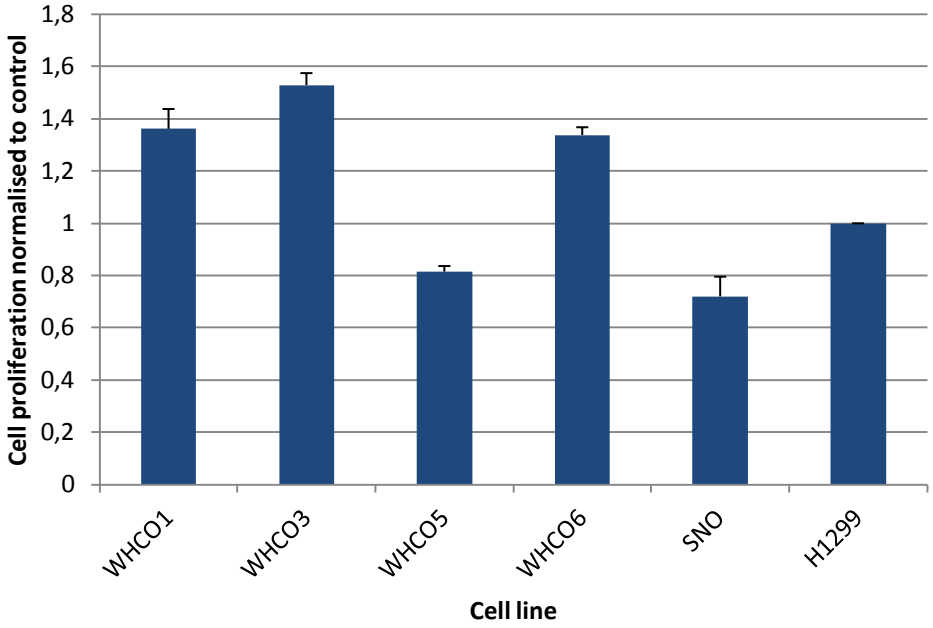

Figure 4.5.1. HOSCC cells reveal high levels of baseline cellular proliferation.

MTT cell proliferation assay performed on each HOSCC cell line seeded at 3×10^5 cells per 3.5 cm tissue culture dish and grown under standard tissue culture conditions for 24 hours reveals varying and elevated levels of cell proliferation in each HOSCC cell line with respect to the H1299 NSCLC cell line used as a comparative control, as determined by absorbencies obtained at 570 nm. Note: Data shown is representative of three independent experiments (n = 3).

The most elevated level of cell proliferation was observed in the WHCO3 cell line. Similarly, elevated levels of cell proliferation were noted in the WHCO1 and WHCO6 cell lines. The lowest levels of cell proliferation were observed in the WHCO5, SNO and H1299 cell lines. Consequently, HOSCC cells exhibit elevated cell proliferation and, therefore, aberrant metabolic mechanisms that may contribute to the malignancy and facilitate selective growth advantages.

In the WHCO3 and WHCO6 cell lines, this elevated cell proliferation and metabolism corresponds with elevated levels of both inactive and active GSK3β. Specifically, in the WHCO3 cell line, this corresponded with low levels of β1 integrin receptors and low abundance of activated caspase 3. In the WHCO1 cell line, elevated proliferation corresponded with high abundance of the inactive GSK3β, as well as high abundance of β1 integrin receptors. Conversely, low proliferation in the SNO cell line corresponded with high abundance of both active and inactive phosphorylated forms of GSK3β, yet elevated abundance of β1 integrin receptors. In the WHCO5 cell line, low cell proliferation corresponded with low abundance of both inactivated and activated forms of GSK3β, as well as low abundance of β1 integrin receptors. Consequently, the modulation of proliferative advantages in HOSCC may be regulated by β1 integrin receptors and GSK3β.

In addition to MTT cell proliferation assays, Trypan Blue cell viability assays provide a measure of cell death and consequently cell survival. Shown in Figure 4.5.2, Trypan Blue cell viability assays performed on HOSCC cells under non-stimulated conditions revealed differential levels of cell death in each cell line.

Overall, all HOSCC cell lines exhibited lower levels of cell death in comparison to the H1299 control cell line. As a result, the HOSCC cells exhibit higher overall survival and viability. This lower overall cell death corresponds with overall lower levels of cleaved and activated caspase 3 compared to the H1299 control, suggesting that the HOSCC cell lines exhibit greater cell survival in comparison to the H1299 control. The WHCO6 cell line exhibited the lowest level of cell death, and therefore the highest cell viability. Following this, the WHCO3 and WHCO1 cell line exhibited low levels of cell death and thus increased viability. The H1299 control cell line exhibited the highest level of cell death and therefore the lowest viability in comparison.

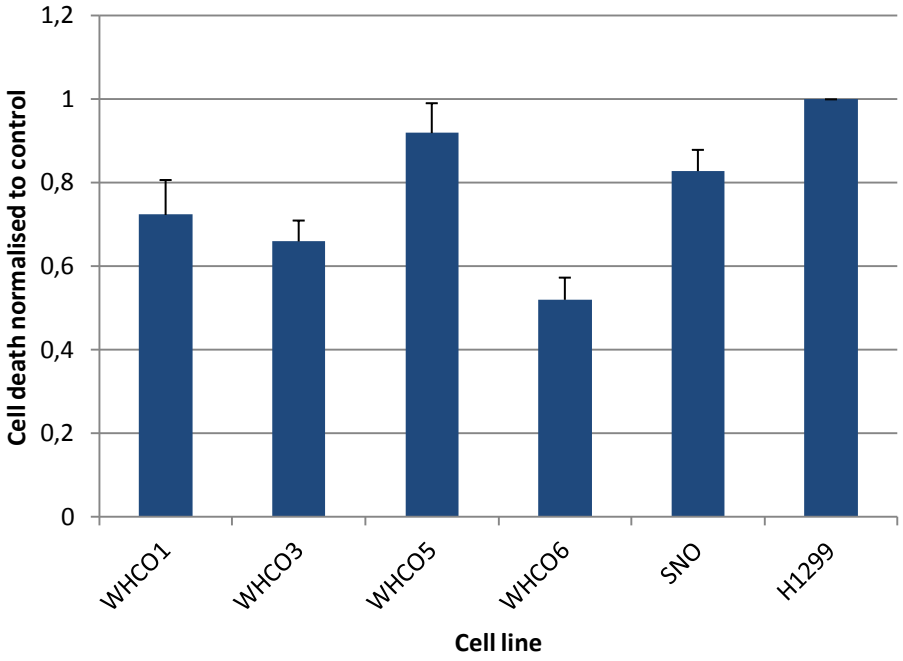

Figure 4.5.2. HOSCC cells exhibit differential levels of cell death and viability under standard conditions.

Trypan Blue cell viability assay performed on each HOSCC cell line seeded at 3×10^5 cells per 3.5 cm tissue culture dish reveals varying levels of cell viability and therefore cell death in each HOSCC cell line after 24 hours under standard, non-stimulated conditions with respect to the H1299 NSCLC cell line used as a comparative control. Note: Data shown is representative of three independent experiments (n = 3).

4.6 Abrogation of GSK3β contributes to selective growth and survival advantages in HOSCC

GSK3β is a Ser/Thr kinase that is constitutively active under normal conditions, and is regulated by phosphorylation of residue Ser-9 by upstream interactors, leading to inhibition of its activity (Frame and Cohen, 2001). The role of inactive GSK3β in the regulation of survival signalling and the regulation of cell death appears contradictory, having been shown to function as both a pro-survival or tumour suppressing module, depending on the cellular context. In leukaemia cells, it has been found that the inhibition of GSK3β using the GSK3β-specific small molecule inhibitor AR-A014418 results in the induction of apoptosis and thus inactivating GSK3β contributes to diminished cell survival (Mirlashari *et al*., 2012). Conversely, in breast cancer cells, inactivation of GSK3β using the small molecule selective GSK3β inhibitor AR-A014418 has been found to repress the expression of tumour suppressors, thereby functioning in pro-survival signalling (Ko *et al*., 2016).

To evaluate the significance of inactive GSK3β in the regulation of survival signalling in HOSCC, the activity of GSK3β was abrogated using the GSK3β-specific inhibitor AR-A014418, which inhibits GSK3β in an ATP-competitive manner. For all following sections, the WHCO3 and WHCO6 cell line were excluded from experimentation, due to their overall elevated abundance of both active and inactive GSK3β. Consequently, all subsequent experimentation was performed on the WHCO1, WHCO5, SNO and H1299 cell lines, using the WHCO6 cell line as an internal control in order to allow for appropriate comparison between immunoblots.

4.6.1 Abrogation of GSK3β activity diminishes the abundance of active caspase 3 and increases adhesion in HOSCC

Immunoblot analysis was performed in order to assess the effect of the specific abrogation of GSK3β activity on the abundance of both inactive GSK3β and HOSCC cell survival as indicated by the abundance of cleaved executioner caspase, caspase 3 using the GSK3β-specific inhibitor AR-A014418. Following western immunoblotting, shown in Figure 4.6.1a and subsequent densitometric evaluation, it was revealed that inhibition of GSK3β activity resulted in an overall increase in abundance of β1 integrin and decreased abundance of cleaved caspase 3, as represented by percentage change in Figure 4.6.1b.

a)

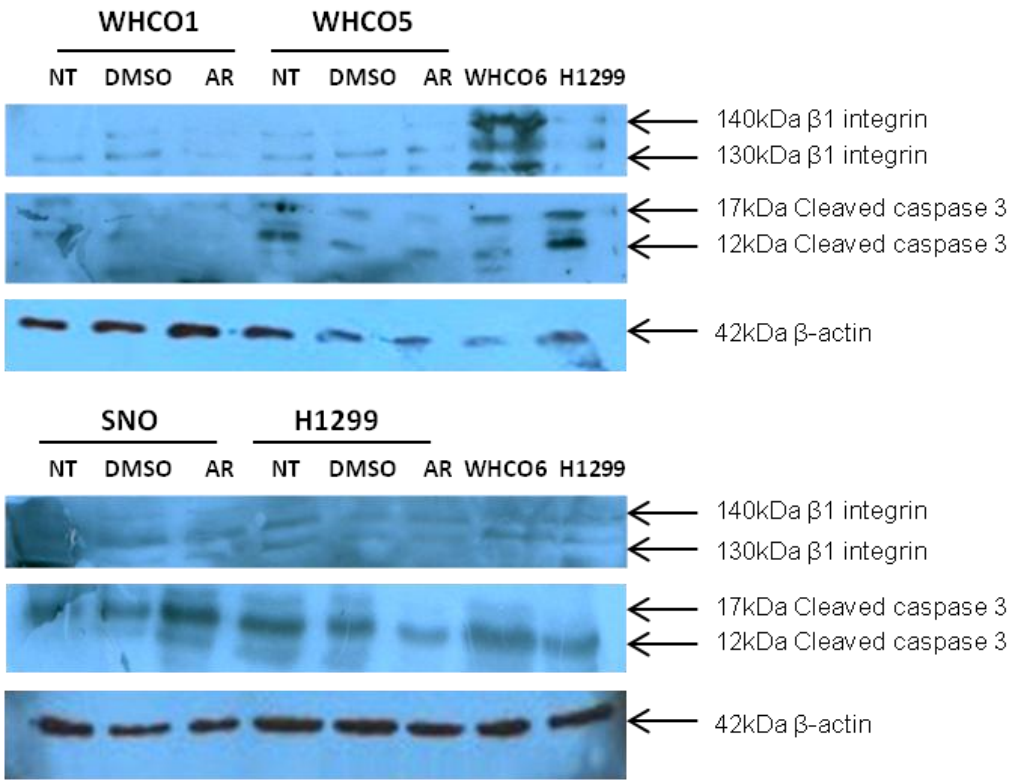

b)

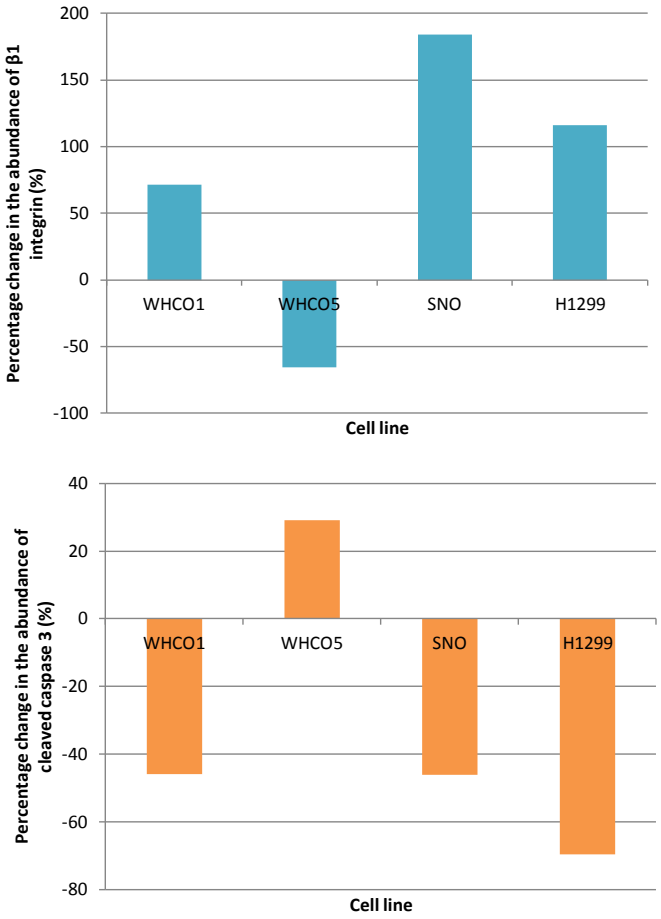

(Note: Figure legend on following page)

Figure 4.6.1. Specific abrogation of GSK3β activity increases the abundance of β1 integrin receptors and a decrease in levels of activated caspase 3 in HOSCC cells.

a) Western immunoblots performed on whole-cell lysates extracted from moderately differentiated HOSCC cells following specific abrogation of GSK3β activity using a GSK3β-specific inhibitor (AR-A014418) for 24 hours and separated on a 10% SDS-PAGE gel. b) Following densitometric evaluation performed on the 130 kDa and 12 kDa bands on th resultant immunoblots using ImageJ, percentage change was calculated using untreated and treated sample values and revealed an increase in overall abundance of β1 integrin receptors, as well as a decrease in the abundance of cleaved caspase 3 in the HOSCC cells following specific abrogation of GSK3β activity. The WHCO6 cell line was utilised as an internal control, and the H1299 cell line was used as a comparative control cell line. The experiment was performed in triplicate (n = 3).

(Note: NT = Untreated, DMSO = DMSO-only control, AR = AR-A014418)

As indicated in Figure 4.6.1b, the abundance of β1 integrin receptors appeared to significantly increase in HOSCC cells following the specific abrogation of GSK3β activity. The greatest increase in β1 integrin abundance was observed in the SNO cell line, exhibiting a 184% increase in abundance in comparison to when grown on standard tissue culture dishes. Similarly, the H1299 cell line exhibited a considerable increase in the abundance of β1 integrin receptors, showing a 116% increase. The WHCO1 cell line also exhibited an increase in the abundance of β1 integrin receptors, illustrating a 72% increase in abundance in comparison to the untreated control. Conversely, in the WHCO5 cell line, a considerable decrease in the expression of β1 integrin receptors was observed, with a 66% decrease in β1 integrin receptors.

Shown in Figure 4.6.1b, specific abrogation of GSK3β activity results in the overall decrease in the abundance of cleaved caspase 3 in HOSCC cells. The greatest reduction in cleaved caspase 3 abundance was observed in the H1299 cell line, with a 70% decrease in the level of cleaved caspase 3 in comparison to the untreated control. The WHCO1 and SNO cell line exhibited a similar decrease in the abundance of cleaved caspase 3, with a 46% decrease in abundance, respectively. Again, the WHCO5 cell line appeared contrary, showing a 29% increase in the abundance of cleaved caspase 3 following specific abrogation of GSK3β activity.

4.6.2 Abrogation of GSK3β activity enhances proliferation and cell viability in HOSCC

GSK3β has more predicted substrates than any other kinase, and therefore is suggested to be involved in the regulation of almost every cellular process, including pathways involved in cellular metabolism and proliferation, however; remains to be elucidated in specific cell types and cellular contexts (Linding *et al.*, 2007). Further, considering altered regulation of metabolism probably occurs in order to maintain the high energy demand for enhanced proliferation in malignancies (Luengo *et al.*, 2017), and therefore contribute to cancer cell survival, the role of inactive GSK3β in these processes was investigated.

It was revealed that following the specific abrogation of GSK3β activity with a GSK3β-specific inhibitor (AR-A0144218) for 24 hours, all HOSCC cell lines experienced an increase in cell proliferation as determined by MTT cell proliferation assays, seen in Figure 4.6.2a. Inhibition of GSK3β activity appeared to markedly increase cellular proliferation in the WHCO1 and SNO cell lines, exhibiting a 41% and 37% increase in proliferation, respectively. The WHCO5 cell line, however, experienced a minimal 7% increase in proliferation following specific abrogation of GSK3β activity. Interestingly, the H1299 control cell line experienced a decrease in cell proliferation by 17% in comparison to the untreated control.

As mentioned previously, GSK3β may directly regulate cell death and viability through the modulation of intermediates involved in cell survival, such as Bmi1 which contributes to cancer stem cell renewal in glioblastoma, caspases, and the proto-oncogene c-myc (Korur *et al.*, 2009; Sun *et al.*, 2008; Kotliarova *et al.*, 2008). Following the specific abrogation of GSK3β activity for 24 hours using the GSK3β-specific inhibitor AR-A014418, Trypan Blue cell viability assays were performed, as indicated in Figure 4.6.2b, and it was found that following the specific inhibition of GSK3β activity, all cell lines experienced a reduction in cell death and thereby an increase in cell viability and survival. The most considerable decrease in cell death was observed in the WHCO5 cell line, exhibiting a 34% decrease in cell death. A 17% decrease in cell death was observed in the WHCO1 cell line following the inhibition of GSK3β activity. In the SNO and H1299 cell lines, abrogation of GSK3β activity appeared to minimally decrease cell death, exhibiting a 0.3% and 8% decrease in cell death, respectively.

a)

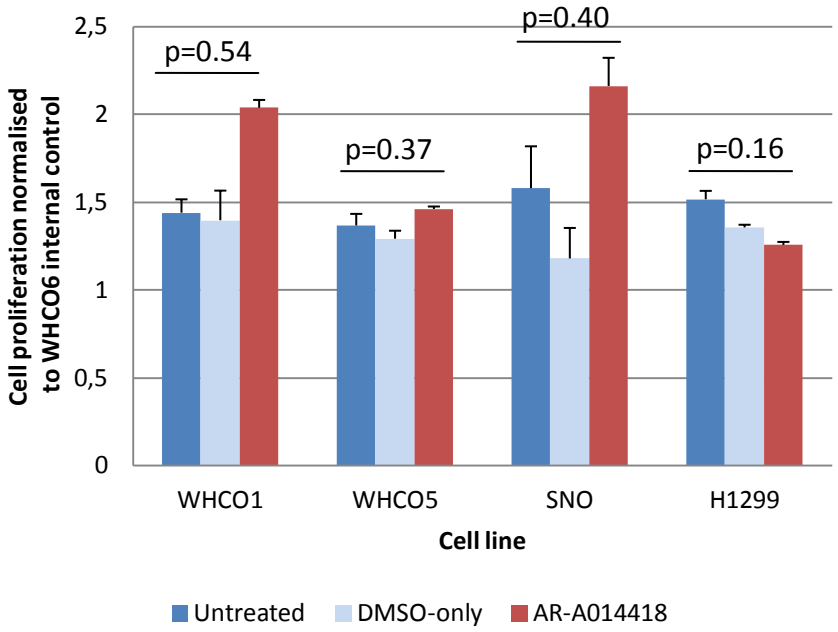

b)

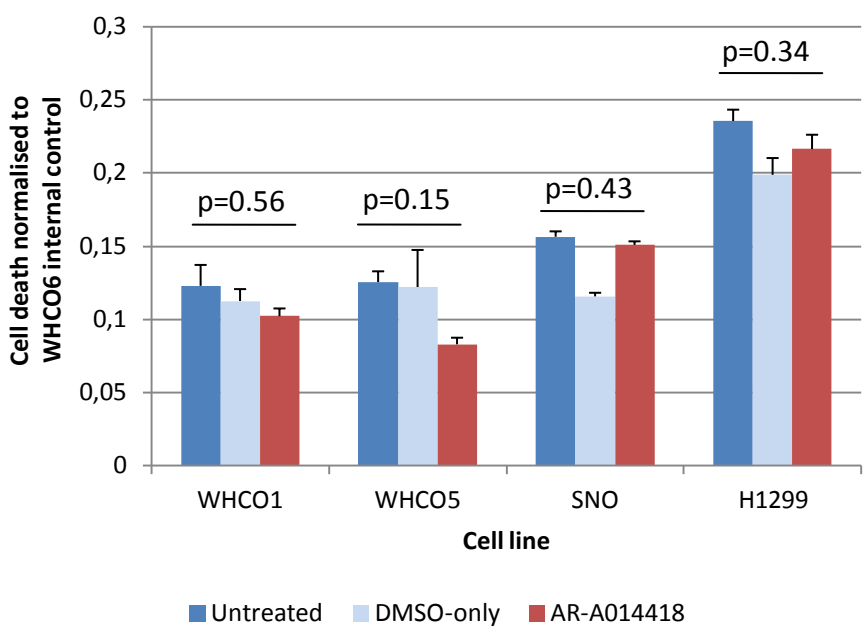

Figure 4.6.2. Specific inhibition of GSK3β activity increases cellular proliferation and diminishes cell death in HOSCC cells.

a) MTT cell proliferation assay performed on each HOSCC cell line seeded at 3 × 105 cells per 3.5 cm tissue culture dish in response to the specific abrogation of GSK3β activity with the GSK3β-specific inhibitor AR-A014418 reveals an overall increase in levels of cell proliferation in each HOSCC cell line after 24 hours. The WHCO6 cell line was used as an untreated internal control in order to allow for comparative analysis with baseline immunoblots. b) Trypan Blue cell viability assay performed on each HOSCC cell line seeded at 3×10^5 cells per 3.5 cm tissue culture dish revealed decreased levels of cell death in each HOSCC cell line after 24 hours following specific inhibition of GSK3β activity using the GSK3β-specific inhibitor AR-A014418 with respect to the untreated WHCO6 cell line used as a comparative internal control. Note: Data shown is representative of three independent experiments (n = 3).

4.7 Constituents of the extracellular matrix modulate survival signalling in HOSCC

Abnormal ECM dynamics are associated with malignant transformation and tumour progression in a number of epithelial cancers. Remodelling of the ECM during malignant transformation and cancer progression including enhanced deposition of ECM constituents such as collagen type I and fibronectin have been noted to occur, and result in modified intracellular signalling (Cox and Erler, 2011). To evaluate the effect of the composition of ECM on GSK3β-mediated adhesion signalling on cancer cell survival, the WHCO1, WHCO5 and SNO cell lines were grown on collagen type I-, as well as fibronectin-coated substrates. Due to the predominant expression of β1 integrin receptors in epithelia compared to other integrin heterodimers, collagen type I and fibronectin were specifically selected for analysis due to their selective binding to β1 integrin receptors.

4.7.1 Collagen type I and fibronectin modulate the adhesion of HOSCC cells

Adhesion of cancer cells to ECM is a mechanistically important step in the development and progression of malignancies. Loss of cell-ECM adhesion facilitates the ability of the cells to detach from the basement membrane and metastasise, whereas establishment of new cell-ECM contacts leads to stabilised interactions between the actin cytoskeleton and surrounding extracellular environment, as well as altered intracellular signalling which drives growth and survival advantages (Okegawa *et al*., 2004). Therefore, understanding the adhesion dynamics of cancer cells with respective ECM may elucidate the role of specific ECM components, as well as the dependency of epithelial malignancies on cell-ECM attachment on survival and progression. Consequently, HOSCC cells were grown on a collagen type I-, and fibronectin-rich substrate for 24 hours and subject to a Crystal Violet cell adhesion assay, shown in Figure 4.7.1, and revealed differential levels of cell adhesion. However; it is important to note that coating of the tissue culture dishes with specific ECM substrate limits the available binding sites for non-collagen type I- and non-fibronectin-binding integrin receptors.

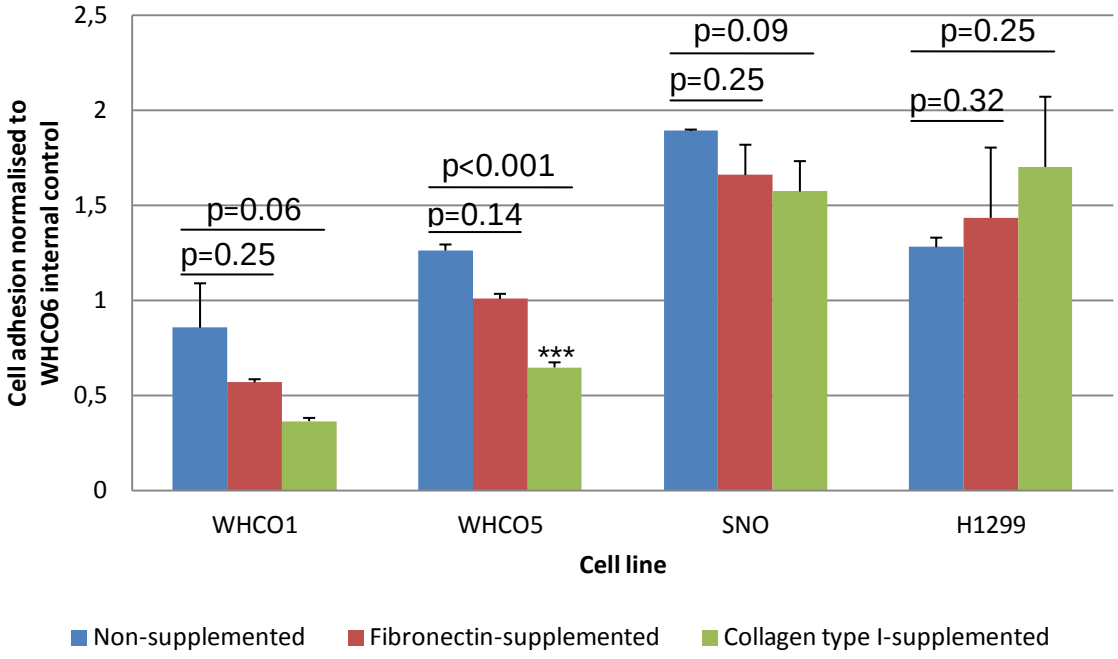

Figure 4.7.1. Collagen type I and fibronectin appear to decrease cellular adhesion of HOSCC cells.

Crystal violet qualitative cell adhesion evaluation performed on each HOSCC cell line seeded at 3×10^5 cells per 3.5 cm tissue culture dish and grown on a collagen type I-, and fibronectin-rich substrate reveals varying and diminished levels of cell adhesion in each HOSCC cell line after 24 hours using the WHCO6 cell line as a comparative control not subject to growth on ECM-coated substrate in order to compare with baseline immunoblots. Note: n = 3.

Illustrated in Figure 4.7.1, it was observed that HOSCC cells grown on an ECM-supplemented substrate exhibit modified adhesion. An overall decrease in adhesion was observed between cells grown on either collagen type I or fibronectin, however; this is due to limiting the number of binding sites available for cell-ECM attachment to occur. It was found that fibronectin increased the adhesion in HOSCC cells at an average of 20% greater adhesion to fibronectin than the cells grown on collagen type I. Conversely, the H1299 cell line exhibited the highest adhesion to collagen type I as an ECM substrate than fibronectin.

4.7.2 Collagen type I and fibronectin increase the abundance of inactive GSK3β in HOSCC

Dysfunction of intracellular signalling pathways contributing to cancer development, progression and survival due to compositional alterations in ECM are largely influenced by outside-in and inside-out signalling mediated by integrin receptors. Specifically, increase in tensile stress as a result of increased tissue stiffness due to enhanced deposition of collagen type I as well as fibronectin has been illustrated to contribute to the malignant phenotype in a number of epithelial cancers including breast cancer (Rudnick and Kuperwasser, 2012). In order to determine the role of ECM on the regulation of GSK3β, specifically inactivation, and therefore the role of GSK3β in integrin-mediated outside-in signalling on HOSCC cell survival, western immunoblotting was perfomed on HOSCC cells grown on a collagen type I-, and fibronectin-rich substrate, indicated in Figure 4.7.2a. Subsequently, densitometric evaluation was performed on the resultant immunoblots and percentage change calculated, as shown in Figure 4.7.2b, and revealed an overall increase in the abundance of inactive GSK3β in all HOSCC cell lines.

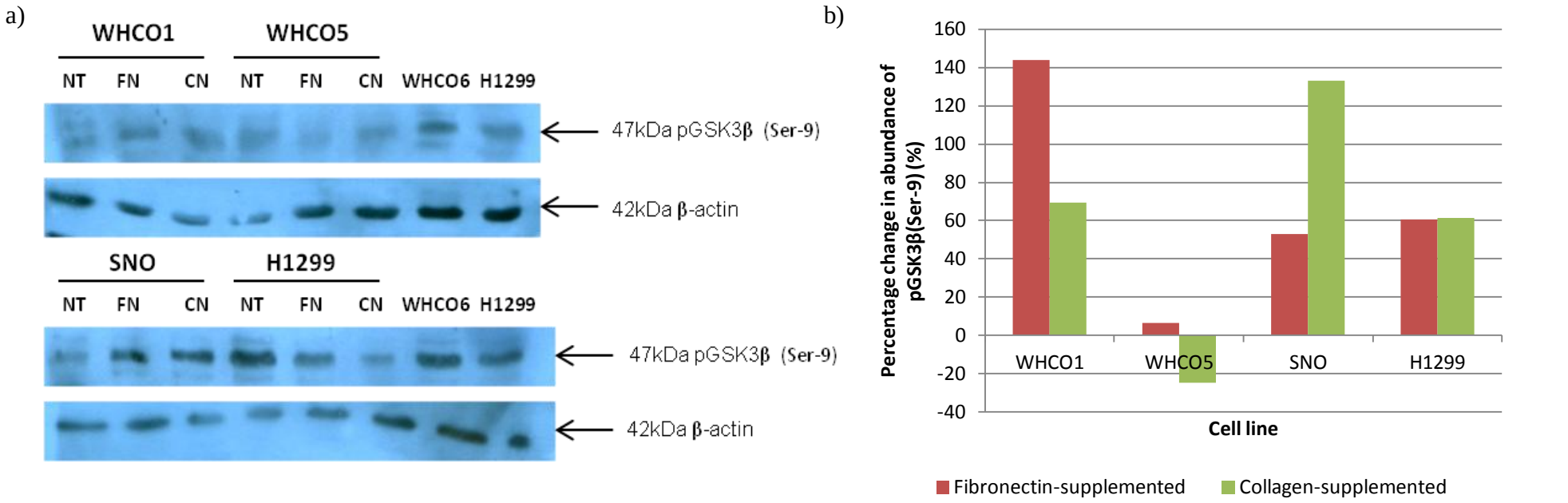

Figure 4.7.2. Collagen type I and fibronectin increase the abundance of inactive GSK3β in HOSCC cells.

a) Western immunoblotting performed on HOSCC whole-cell lysates grown on a collagen type I-, and fibronectin-coated substrate for 24 hours separated on a 10% (w/v) SDS-PAGE gel show variances in the abundance of inactive GSK3β in comparison to the cells grown on standard tissue culture dishes using the WHCO6 cell line not grown on ECM substrate as a comparative control. b) Following immunoblotting, densitometric evaluation was performed and percentage change in the level of inactive GSK3β was calculated, revealing an overall increase in the abundance of inactive GSK3β when grown on ECM (n = 3). (Note: NT = Untreated, FN = Fibronectin, CN = Collagen type I)

Following the growth of HOSCC cells on a collagen type I-, and fibronectin-supplemented substrate, it was found that there was an overall increase in the expression of inactive GSK3β in comparison to the HOSCC cells grown on standard tissue culture dishes. When grown on a fibronectin-rich substrate, the greatest increase in abundance of inactive GSK3β was observed in the WHCO1 cell line, with a 144% increase in abundance. A similar increase in abundance of inactive GSK3β was observed in the SNO and H1299 cell lines, exhibiting a 53% and 60% increase in the level of inactive GSK3β, respectively. The lowest increase in abundance of inactive GSK3β was observed in the WHCO5 cell line.

Interestingly, when grown on a collagen type I-rich substrate, a decrease in the abundance of inactive GSK3β was seen in the WHCO5 cell line. Conversely, a significant increase in the level of inactive GSK3β was observed in the WHCO1, SNO and H1299 cell lines, exhibiting a 69%, 133% and 61% increase in abundance, respectively.

4.7.3 Collagen type I and fibronectin differentially influence proliferation and viability in HOSCC cells

To evaluate the effects of ECM constituents on cell behaviour that contributes to cancer cell survival by means of selective growth advantages, HOSCC cells were grown on both collagen type I- and fibronectin-supplemented substrate in order to observe alterations in cellular proliferation, as well as cell death.

From Figure 4.7.3a, it can be observed that collagen type I more significantly affects the proliferation of HOSCC cells than fibronectin in comparison to the HOSCC cells grown under standard tissue culture conditions. Overall, the cells grown on either a collagen type I- or fibronectin-rich substrate exhibited a decrease in cellular proliferation, although as aforementioned is due to the limited combination of integrin heterodimers available for binding to the substrate. However, it is noted in the SNO and H1299 cell lines, a significant increase in proliferation was observed with a 65% and 54% increase, respectively in comparison to cells grown in absence of collagen type I and fibronectin. Growth on fibronectin appeared to minimally influence proliferation in all HOSCC cell lines, with the greatest decrease in proliferation (–12%) observed in the WHCO1 cell line.

Again, illustrated in Figure 4.7.3b, it was found that growth of HOSCC cells on ECM-rich substrates resulted in an overall increase in cell death. As previously mentioned, selectively coating the tissue culture dishes with a single substrate being collagen type I and fibronectin, respectively, limits cell adhesion to the substrate with collagen type I-, and fibronectin-binding integrin receptors only. As a result, the variances in cell death will be compared between substrates and not between experimental and control conditions. From Figure 4.7.3b, it was observed that growth on a collagen type I-rich substrate significantly increased levels of cell death in the WHCO1 cell line in comparison to growth on a fibronectin-rich substrate by 53%. Similarly, the H1299 cell line appeared to have more increased levels of cell death when grown on a collagen-supplemented substrate versus a fibronectin-supplemented substrate. In contrast, the WHCO5 and SNO cell lines exhibited more cell death when grown on a fibronectin-rich substrate. Therefore, it is apparent that an ECM rich in collagen type I similarly influences HOSCC cell viability more significantly than fibronectin.

a) b)

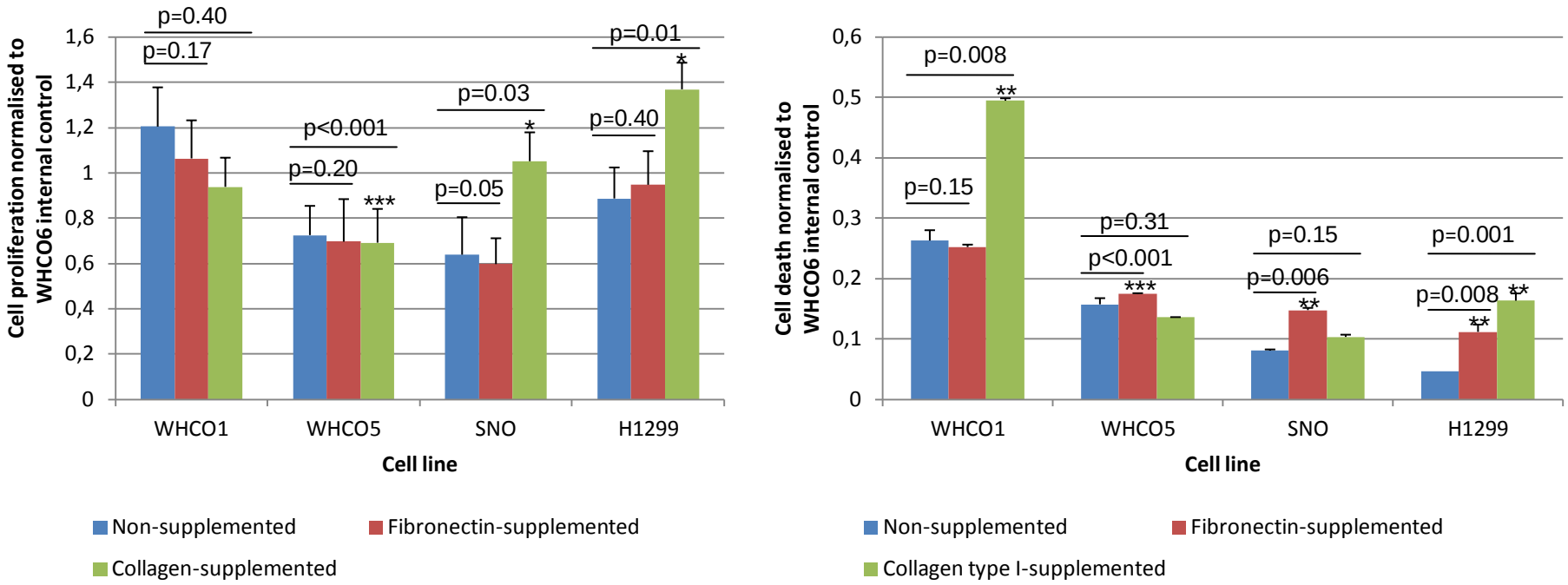

Figure 4.7.3. Collagen type I and fibronectin differentially influence cellular proliferation and cell death in HOSCC cells.

a) MTT cell proliferation assay performed on each HOSCC cell line seeded at 3×10^5 cells per 3.5 cm on collagen type I-, and fibronectin-coated tissue culture dishes after 24 hours. The WHCO6 cell line was used as an internal control in order to allow for comparative analysis. b) Trypan Blue cell viability assay performed on each HOSCC cell line seeded at 3×10^5 cells per 3.5 cm tissue culture dishes coated with collagen type I and fibronectin, respectively and grown for 24 hours using the WHCO6 cell line as internal comparative control grown on standard tissue culture dishes in order to compare with densitometry obtained from baseline immunoblots (n = 3).

CHAPTER 5: Discussion

The elucidation of the molecular mechanisms underpinning the development and progression of many epithelial malignancies has largely focused on the intrinsic features of the malignancy, such as aberrations in gene expression, however; in recent years, it has become increasingly evident that communication between cancer cells and the extrinsic environment plays a mechanistically important role in the process of tumourigenesis and the maintenance of cancer cell survival (Wu *et al*., 2018). In particular, the adhesive communication between cell and constituents of the ECM has been illustrated to strongly contribute to the pathogenesis of epithelial malignancies. Central to cell-ECM communication are transmembrane integrin receptors which facilitate the perception of alterations in the local extracellular environment of the cell and relay the signals into the cell, triggering the activation of intracellular signalling pathways thereby eliciting selective growth and survival responses.

Facilitating the transmission of these extrinsically-originating signals are intracellular signalling interactors, such as ILK and FAK localised at focal adhesion sites on the cytoplasmic side of the integrin receptors. ILK and FAK then regulate downstream interactors, including GSK3β. Shown to regulate a multitude of intracellular processes, such as proliferation, metabolism, apoptosis and survival, GSK3β has become a significant focus as a potential therapeutic target for a number of pathological conditions including cancer. As a consequence, cell-ECM signals may converge at GSK3β, although the role of GSK3β in these pathways remains poorly understood. Furthermore, the roles of GSK3β in epithelial malignancies, and the maintenance of survival thereof, remain largely under-investigated. As such, elucidating the importance of GSK3β in cell-ECM communication, as well as survival signalling in HOSCC and other epithelial malignancies may highlight the necessity to focus on the interplay between intrinsic and extrinsic factors that contribute to cancer development and progression.

5.1 GSK3β appears to be differentially regulated in HOSCC

Under normal conditions, GSK3β remains constitutively active and is regulated through phosphorylation by upstream interactors at two main phosphorylation sites, Ser-9 and Tyr-216. As previously mentioned, phosphorylation of GSK3β at Ser-9 leads to inhibition of its activity, whereas phosphorylation at Tyr-216 results in enhanced activation. However, the

role of both phospho-forms in survival signalling in epithelial malignancies remains contradictory. Western immunoblot and densitometric analyses revealed that both inactive and active phosphorylated forms of GSK3β are present in the HOSCC cell lines. In comparison to the H1299 control cell line, which is a known overexpressor of GSK3β (Zeng *et al*., 2014), it was found that an elevated abundance of inactive GSK3β (pGSK3β (Ser-9)) was present in all HOSCC cell lines, with the exception of the WHCO5 cell line. Interestingly, the abundance of active GSK3β (pGSK3β (Tyr-216)) exhibited similarly elevated levels in each HOSCC cell line in comparison to the H1299 control cell line again with the exception of the WHCO5 cell line.

Consequently, it is apparent that HOSCC cells favour neither phosphorylated form of GSK3β for cell survival. Therefore, it may be likely that interplay between both inactive and active phospho-forms in survival signalling exists in HOSCC, and that the regulation of GSK3β in HOSCC may occur differentially according to survival demands during the progression of the malignancy. Evidence that this interplay exists between both phosphorylated forms of GSK3β in cancer cell survival has been illustrated in ovarian cancer cells, whereby expression levels of both pGSK3β (Ser-9) and pGSK3β (Tyr-216) appeared similar, and appeared to contribute to resistance to cisplatin therapies through stabilisation of the tumour-suppressor p53 due to elevated pGSK3β (Ser-9) and advanced disease progression as a result of elevated levels of pGSK3β (Tyr-216) (Cai *et al*., 2007; Fu *et al*., 2014).

5.2 β1 integrin receptors are necessary for adhesion of HOSCC cells to substrate

Appropriate communication between epithelial cells and the surrounding extracellular environment is not only fundamental to the differentiation, development and organisation of epithelial tissue, but is additionally critical for epithelial cell homeostasis. Communication is facilitated by the establishment of adhesive contacts between the cell and ECM by transmembrane integrin receptors. Particularly important for the structural and functional maintenance of the epithelial tissue phenotype are β1 integrin receptors. Specifically, β1 integrin receptors are the main drivers of epithelial cell polarity and angiogenesis, whereby abrogation of β1 integrin receptors has been illustrated to result in a myriad of structural and behavioural defects. Further emphasising the importance of β1 integrin receptors in the structure and function of epithelial tissue, it has been found that genetic deletion of β1 integrin receptors in mammary epithelial cells has been shown to lead to a loss in polarity, as well as a loss in attachment to the basement membrane (Akhtar and Streuli,

2013). In addition to this loss of tissue organisation and structure in the absence of β1 integrin receptors, abrogation of expression of β1 integrin receptors in mammary epithelial cells abolishes appropriate functionality of the tissue, resulting in defective prolactin signalling (Naylor *et al*., 2005).

Furthermore, dysfunction of appropriate adhesive cues mediated by β1 integrin receptors contributes to the malignant transformation of epithelia (Läubli and Borsig, 2019). This has been documented in prostate cancers, where sustained activation of β1 integrin receptors contributes to the initiation and development of the disease (Lee *et al*., 2014). The abundance of β1 integrin receptors was investigated, and it was observed that an overall elevated level of β1 integrin receptors was present in HOSCC cells. As a result, β1 integrin receptors may facilitate the development and progression of HOSCC. The most abundant level of β1 integrin receptors was detected in the WHCO1 cell line, displaying a higher level of β1 integrin receptors than in the H1299 control cell line. A similar yet still elevated abundance of β1 integrin receptors was noted in the WHCO6 and SNO cell lines. Conversely, both the WHCO3 and WHCO5 cell lines exhibited low levels of β1 integrin receptors.

Thus, these observations suggest that elevated levels of β1 integrin are required by HOSCC cells to facilitate survival and maintenance of the malignancy, and β1 integrin receptors are responsible for facilitating adherent communication between HOSCC cells and the surrounding extracellular environment. Overexpression of β1 integrin receptors has similarly appeared to be important in the mechanistic progression of other epithelial malignancies, involved in processes such as proliferation, invasion, metastasis and survival (Pan *et al*., 2018). However, due to the low abundance of β1 integrin receptors in both the WHCO3 and WHCO5 cell lines, it is apparent that other integrin receptors may therefore serve to facilitate cell–ECM communication in HOSCC.

In particular, it has been found that β3 integrin receptors similarly facilitate epithelial cancer cell adhesion to surrounding ECM, and have been documented to play a role in tumour initiation and cancer cell survival in prostate cancers (Desgrosellier and Cheresh, 2010). Further, in pancreatic cancer cells, β3 integrin receptors have been noted to contribute to cancer cell survival through the activation of Src, and the expression of β3 integrin was found to be a marker of aggressiveness of the malignancy (Desgrosellier *et al*., 2009). Therefore, in the WHCO3 and WHCO5 cell lines, β3 integrin receptors may be predominant when compared to β1 integrin receptors in adhesion-mediated survival signalling. However,

considering detection of β3 integrin receptors was not performed in this study, it could be likely that β1 integrin receptors and β3 integrin receptors are expressed concomitantly in HOSCC, thereby contributing to survival and progression of the disease.

In addition to the detection of the 130 kDa β1 integrin polypeptide, a 140 kDa β1 integrin isoform was detected in each of the HOSCC cell lines. The 140 kDa β1 integrin isoform is indicative of *N*-glycosylated β1 integrin. As a result, *N*-glycosylation of β1 integrin receptors in HOSCC may facilitate β1 integrin complex formation and thereby sustain β1 integrin-mediated survival signalling. This *N*-glycosylation of β1 integrin has been illustrated to function in cell migration, as well as facilitate the activation of β1 integrin (Hou *et al.*, 2014). Furthermore, hyperglycosylation of β1 integrin has been noted to suppress immune responses in cancer development and promote invasion and metastasis (Läubli and Borsig, 2019).

5.3 Caspase 3 is positively regulated by GSK3β in HOSCC and elicit non-apoptotic functions

One of the major hallmarks of cancer is the ability of the cancer cells to evade and resist cell death in the form of apoptosis (Hanahan and Weinberg, 2011). Responsible for the induction of the execution step of apoptosis which ultimately drives cell death is caspase 3. Upon the perception of a cellular stress signal, apoptotic signalling cascades are initiated and executed following the proteolytic cleavage of caspase 3 into its functional and activated subunits. Detection of cleaved caspase 3 was used as a measure of the resistance to cell death in HOSCC, as tumour cells exhibit aberrant apoptotic signalling and dysfunctional activation of caspase 3 to elicit cancer cell survival.

It was found that the HOSCC cell lines exhibited an overall lower abundance of cleaved and activated caspase 3 in comparison to the H1299 control cell line, and corresponding with overall greater levels of cell viability, indicated by lower levels of cell death, as determined by Trypan Blue cell viability assays. However, with respect to the control, levels of cleaved caspase 3 were still elevated. Usually an indicator of the induction of apoptosis, these data appear contradictory as tumour cells specifically evade cell death in order to facilitate selective growth and survival advantages. Interestingly, in the WHCO1, WHCO6 and SNO cell lines, an increase in cleaved caspase 3 was found to correspond to both an elevated level of β1 integrin receptors, as well as an elevated level of inactive GSK3β (pGSK3β (Ser-9)). This may be indicative that β1 integrin pathways mediated by inactive GSK3β increase the

initiation of apoptotic events in HOSCC. However, this positive regulation of caspase 3 leading to its activation may serve as a more useful tool in maintaining survival and proliferative signalling in HOSCC. Surprisingly, it has been found that levels of apoptosis appear more elevated in invasive breast carcinomas in comparison to normal mammary epithelium, and that these rates additionally corresponded with greater levels of cellular proliferation (Bai *et al.*, 2001; Parton *et al.*, 2002).

Consequently, caspase 3 may be involved in non-apoptotic signalling in HOSCC, and regulated positively by β1 integrin/GSK3β pathways in the WHCO1 and WHCO6 cell lines. This is corroborated by the observation of cellular proliferation in HOSCC, whereby elevated proliferation was noted in the WHCO cell line series as determined by MTT cell proliferation assays. Therefore, in HOSCC the positive regulation of caspase 3 stimulates growth and proliferation. Studies have indicated that the stimulation of proliferation by activated caspase 3 in invasive malignancies may be a result of the upstream regulation of prostaglandin E_2 (PGE_2) by caspase 3 (Huang *et al.*, 2011). PGE_2 then regulates cyclooxygenase-2 (COX2) downstream, contributing to proliferation-, and survival-relevant inflammatory signalling (Lang *et al.*, 2017). Similarly, cleaved caspase 3 has been reported to regulate the activity of calcium-independent phospholipase A_2 ($iPLA_2$), again stimulating the expression of PGE_2 in lung cancers (Iitake *et al.*, 2015). Elevated expression of cleaved caspase 3 has additionally been shown to correlate with lower overall prognosis in gastric cancers (Hu *et al.*, 2014), indicating that the activation of caspase 3 in HOSCC cells may serve to induce a compensatory survival mechanism which triggers higher rates of cellular proliferation in order to facilitate the progression of the malignancy. Consequently, non-apoptotic functionality of caspase 3 appears to play a significant role in the maintenance of selective growth advantages in HOSCC, as well as other epithelial malignancies.

5.4 Inactive GSK3β plays a pivotal role in inside-out signalling and survival-relevant signalling in HOSCC

The regulation of GSK3β in epithelial malignancies appears to be a fundamental mechanism in the maintenance of the disease, whereby both phosphorylated forms of GSK3β are likely involved in the modulation of multiple signalling pathways contributing to proliferative and survival advantages. However, it was found that, with specific reference to adhesion-mediated survival signalling, inactive GSK3β (pGSK3β (Ser-9)) may play a more significant role in these pathways in HOSCC. This was noted through observing elevated levels of

β1 integrin receptors and elevated levels of cleaved caspase 3 in those cell lines exhibiting elevated levels of inactive GSK3β. Consequently, the effect of abrogating the activity of GSK3β in HOSCC on survival signalling and adhesion signalling was analysed.

Following immunoblot analyses, it was found that abrogation of GSK3β activity increased the overall expression of β1 integrin receptors in HOSCC cells. Conversely, abrogation of GSK3β activity resulted in diminished expression of cleaved caspase 3. These findings suggest that inactivation of GSK3β results in the activation of inside-out cascades and results in the stimulation of the expression of β1 integrin receptors in HOSCC. As β1 integrin receptors have been illustrated to contribute to cancer cell survival through the activation of the NF-κB pathway, inactivation of the tumour suppressor p53, as well as increased expression of the pro-survival Bcl-2 (Nam *et al.*, 2013; Martin *et al.*, 2012; Popov *et al.*, 2011), it is likely that the observed increase in the abundance of β1 integrin receptors following inhibition of the activity of GSK3β contributes to the regulation of these pathways in HOSCC. Moreover, it may be likely that the inactivation of GSK3β triggers resistance to therapeutics in HOSCC as a result of enhancing β1 integrin receptor abundance. This has been observed in breast cancers, whereby the expression of β1 integrin receptors results in diminished levels of therapeutic-induced cell death via the regulation of the PI3K/Akt pathway (Aoudjit and Vuori, 2001). Resistance to therapeutics as a consequence of overexpression of β1 integrin receptors has also been observed in NSCLC, whereby resistance to the epidermal growth factor receptor (EGFR) inhibitor gefitinib is conferred by β1 integrins (Ju *et al.*, 2010). Therefore, in HOSCC inactivation of GSK3β may be required for chemoresistance mediated by β1 integrin receptors, thereby increasing the pro-survival effects elicited by β1 integrin receptors. Moreover, as indicated by gefitinib resistance in NSCLC, the overexpression of β1 integrin receptors may additionally function in growth factor crosstalk in HOSCC. Consequently, enhanced β1 integrin signalling as mediated by inactive GSK3β is necessary for increased survival of the malignancy and suggests a β1 integrin/GSK3β pathway exists.

The overall diminished abundance of cleaved caspase 3 following the specific abrogation of GSK3β activity further suggests that inactive GSK3β contributes to survival advantages in HOSCC cells as a result of less induction of apoptotic events. Consequently, a β1 integrin/GSK3β/caspase 3 pathway has been elucidated in HOSCC and contributes to the survival of the malignancy. Further in substantiation of this pathway in HOSCC is such that

the specific abrogation of GSK3β activity resulted in an overall increase in cellular proliferation and an increase in cell viability, as indicated by a lower overall level of cell death. Consequently, inactive GSK3β regulates pathways in HOSCC relevant to establishing proliferative and survival advantages through the modulation of β1 integrin receptors and caspase 3. Additionally, inactivation of GSK3β would trigger the activation of the canonical Wnt pathway contributing to cancer cell survival. In this pathway, inhibitory phosphorylation of GSK3β at Ser-9 leading to its inactivation, subsequently stabilising β-catenin, allowing for the translocation of β-catenin to the nucleus and thereby the transcription of T-cell factor/lymphoid enhancer-binding factor (TCF/LEF) target genes (Wu *et al.*, 2009).

Contrastingly, however; abrogation of GSK3β activity corresponded inversely with the abundance of β1 integrin receptors and cleaved caspase 3 in the WHCO5 cell line. Specific inhibition of GSK3β activity resulted in a decrease in the level of β1 integrin receptors and conversely an increase in cleaved caspase 3. These data additionally corresponded with an increase in cellular proliferation and viability. Consequently, in the WHCO5 cell line, inactive GSK3β enhances the non-apoptotic function of cleaved caspase 3, facilitating growth stimulation and protection against cell death. The decrease in the level of β1 integrin as a result of inactivating GSK3β similarly illustrates that GSK3β plays a fundamental role in inside-out signalling in HOSCC.

5.5 ECM-originating signals converge at GSK3β in HOSCC

As presented in Section 5.4, this research indicates that GSK3β functions in inside-out signalling in HOSCC, contributing to the maintenance of proliferative and survival advantages through modulating the abundance of β1 integrin receptors. To further explore the effects of outside-in signalling on GSK3β-mediated survival signalling in HOSCC, analyses were performed on HOSCC cells following exposure to specific ECM constituents. Following immunoblot analyses, it was found that both collagen type I, and fibronectin notably increase the abundance of inactive GSK3β in HOSCC cells with an over 50% increase in abundance observed. Again, contrasting these findings is the WHCO5 cell line, displaying the least variance in abundance of inactive GSK3β, and specifically a decrease in the abundance of inactive GSK3β on collagen type I.

The integrin receptor predominantly responsible for binding collagen type I and fibronectin is the β1 integrin receptor. Therefore, extrinsic signals in HOSCC are perceived by β1 integrin receptors, initiating outside-in signalling. Activation and clustering of β1 integrin receptors

along the surface of the cell subsequently recruit ILK and FAK as adaptor and scaffolding proteins at the cytoplasmic tail domains of the integrin receptors. Consequently, an increase in the activation of β1 integrin receptors results in an increase in the activity of the adaptor proteins. It has been illustrated that overexpression of ILK contributes positively to the invasive phenotype in malignancies, and is associated with the translocation of β-catenin to the nucleus, facilitating the transcription of TCF/LEF target genes (Novak *et al*., 1998). Considering the involvement of GSK3β on the regulation of β-catenin, as well as the upstream inhibitory regulation of GSK3β by ILK, it is likely then that β1 integrin-mediated signals are transmitted downstream to GSK3β by ILK, in a signalling mechanism proposed in Figure 5. Similarly, FAK appears to play a central role in the modulation of β-catenin, and thereby likely converges extrinsic signals at GSK3β leading to the transcription of TCF/LEF target genes (Zheng *et al*., 2019). Furthermore, FAK has been noted to facilitate sustained mitogen-activated protein kinase (MAPK) signalling through crosstalk between integrin-mediated pathways (Wu *et al*., 2008). As a consequence, ECM-originating signals converge at GSK3β in HOSCC, facilitating outside-in survival signalling.

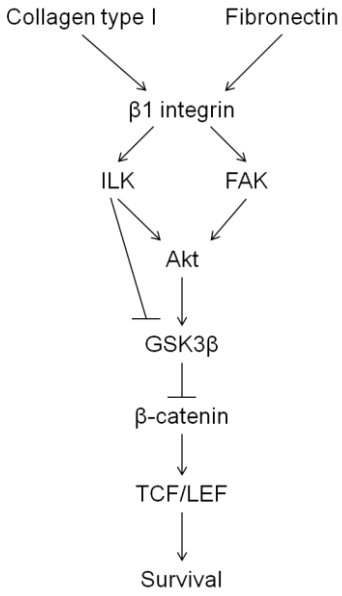

Figure 5. Outside-in survival signals transmitted by β1 integrin receptors likely converge at GSK3β.

Binding of ECM ligands, such as collagen type I and fibronectin to β1 integrin receptors in HOSCC result in the activation and clustering of β1 integrin receptors, which subsequently recruit and activate downstream partners, such as ILK and FAK. These signals then converge at GSK3β, which becomes inactivated through inhibitory phosphorylation at Ser-9, leading to the transcription of TCF/LEF target genes enhancing cellular survival.

5.6 Composition of ECM modulates tumour cell behaviour in HOSCC

Remodelling of the ECM and dysfunctional ECM dynamics has been shown to contribute to the malignant phenotype in epithelial cancers. In recent years, it has been documented that the surrounding tumour microenvironment and composition of the ECM has been illustrated to be a fundamental mechanism in the growth and proliferation of the malignancy (Anari *et al*., 2018). Specifically, enhanced deposition of ECM constituents resulting in increased tissue stiffness has been illustrated be a fundamental mechanism in the development of cancer (Jang *et al*., 2018). The effect of different ECM constituents on HOSCC tumour cell behaviour was evaluated, with specific focus on collagen type I and fibronectin. It was found that collagen type I and fibronectin appeared to differentially effect the adhesion, proliferation, and survival of HOSCC cells.

From the data obtained, it was apparent that HOSCC cells exhibit greater adhesion to fibronectin as a substrate than collagen type I. This observable difference in the extent of adhesion of HOSCC cells on fibronectin versus collagen type I may again be due to the *N*-

glycosylation of the fibronectin-binding α5β1 integrin receptor facilitating cell adhesion (Hou *et al*., 2016). Therefore it has been further substantiated that *N*-glycosylation of β1 integrin receptors occurs in HOSCC and facilitates adhesion-mediated signalling. In addition to cell adhesion, it was found that fibronectin more greatly influences proliferation in HOSCC. Research has indicated that fibronectin modulates proliferation and survival signalling through the activation of the PI3K/Akt signalling pathway in glioma (Liao *et al*., 2018), which is additionally a known upstream negative regulator of GSK3β. Consequently, the same mechanism may exist in HOSCC. Furthermore, due to the enhanced adhesion on fibronectin observed, it is likely that activation of β1 integrin receptors is increased in HOSCC cells when grown on fibronectin rather than collagen type I.

In contrast, cell viability appeared to increase in HOSCC cells when grown on collagen type I versus fibronectin. Accounting for this may be the attachment of collagen type I to the α2β1 integrin receptor. It has been reported that enhanced activation of the α2β1 integrin receptor in response to collagen type I elicits resistance to apoptosis in mammary epithelium (Baeckstroém *et al*., 2000). As a result, increased activation of α2β1 integrin receptors may serve in the increase of cell viability in HOSCC when collagen type I is present as a constituent of the ECM.

More importantly, however; is to note the overall decrease in cell adhesion, cell proliferation and increase in cell death of HOSCC cells when only one type of ECM ligand is present in the local extracellular environment. This is indicative of a complex and dynamic ECM that functions synergistically to facilitate selective growth and survival advantages in HOSCC. These data illustrate that each component of ECM differentially affects the behaviour and physiology of HOSCC cells, and thereby function in the modulation of different intracellular pathways. As a consequence, the development and progression of HOSCC relies on a multifaceted extrinsic environment, where ECM constituents exist concomitantly to promote adhesion-mediated survival signalling.

CHAPTER 6: Conclusion

Elucidating the molecular landscape in epithelial malignancies remains critical not only understanding the nature of the malignancy, but also to allow for the development of more effective therapeutics to improve prognostic outcomes. However, investigation into the molecular mechanisms behind epithelial cancers has predominantly focused on intrinsic features. More evidence has suggested that the local extracellular environment, particularly ECM elicits a significant function in the development and maintenance of the malignant phenotype. This research has revealed that HOSCC relies strongly on adhesive communication between the cell and surrounding environment as regulated by β1 integrin receptors, and the elevated presence of β1 integrin receptors facilitates survival and growth advantages. Moreover, it may be so that the presence of β1 integrin receptors confers resistance to therapies in HOSCC, contributing to the poor prognosis and high invasiveness of the disease.

GSK3β has, in recent years, been shown to have myriad involvement in almost every cellular process, although the specific role and interaction between GSK3β-containing pathways remains poorly elucidated, specifically with reference to specific cell types and signalling environments. It was subsequently revealed that GSK3β influences survival and proliferation in HOSCC. It is apparent that GSK3β is variably regulated, and that both phosphorylated forms are present. Consequently, the regulation of GSK3β may be modulated differentially during progression of the malignancy depending on the required cellular response. It was noted that the level of inactive GSK3β corresponded more notably with the enhanced levels of β1 integrin, thereby illustrating the presence of a β1 integrin/GSK3β pathway in HOSCC. Furthermore, it was observed that inactive GSK3β corresponded with increased levels of cleaved caspase 3, in conjuction with high levels of proliferation and viability. Therefore, in HOSCC, cleaved caspase 3 may elicit non-apoptotic functionality in order to facilitate the survival and progression of the malignancy.

Moreover, inactive GSK3β was found to participate in inside-out signalling, whereby inactivation of GSK3β increased levels of β1 integrin. Additionally, inactive GSK3β resulted in a decrease in cleaved caspase 3, which corresponded with enhanced proliferation and viabilty. As a result, GSK3β appears to play a fundamental role in survival signalling in HOSCC, and exhibits interplay between inside-out and outside-in signalling through the

modulation of β1 integrin receptors. Additionally, HOSCC appears to be highly dependent on a dynamic and complex ECM in order for proliferation and survival. Therefore, GSK3β exhibits multifaceted functionality in HOSCC and regulation of GSK3β appears critical in the maintenance of survival of the malignancy. Furthermore, from this study, GSK3β has been elucidated to play a central role in adhesion-mediated signalling. Consequently, HOSCC is a mechanistically complex disease that requires further elucidation into the molecular landscape, such as possible crosstalk between β1 integrins and growth factor signalling, or the existence of compensatory mechanisms against apoptosis, and specifically the role of GSK3β in these processes.

7. REFERENCE LIST

Abdul-Ghani M, and Megeney L, (2008). Rehabilitation of a Contract Killer: Caspase-3 Directs Stem Cell Differentiation**.** *Cell Stem Cell* **2**: 515–516.

Adams J, and Cory S, (2007). The Bcl-2 apoptotic switch in cancer development and therapy. *Oncogene* **26**: 1324-1337.

Akhtar N, and Streuli C, (2013). An integrin-ILK-microtubule network orients cell polarity and lumen formation in glandular epithelium. *Nature Cell Biology* **15**: 17–27.

Anari F, Ramamurthy C, and Zibelman M, (2018). Impact of tumor microenvironment composition on therapeutic responses and clinical outcomes in cancer. *Future Oncology* **14**: 1409–1421.

Aoudjit F, and Vuori K, (2001). Integrin signaling inhibits paclitaxel-induced apoptosis in breast cancer cells. *Oncogene* **20**: 4995–5004.

Attwell S, Mills J, Troussard A, and Dedhar S, (2003). Integration of cell attachment, cytoskeletal localization, and signaling by integrin-linked kinase (ILK), CH-ILKBP, and the tumor suppressor PTEN. *Molecular Biology of the Cell* **14**: 4813-4825.

Baeckstroém D, Lu P, and Taylor-Papadimitriou J, (2000). Activation of the a2b1 integrin prevents c-erbB2-induced scattering and apoptosis of human mammary epithelial cells in collagen. *Oncogene* **19**: 4592–4603.

Bai M, Agnantis N, Kamina S, Demou A, Zagorianakou P, Katsaraki A, and Kanavaros P, (2001). *In vivo* cell kinetics in breast carcinogenesis. *Breast Cancer Research* **3**: 276-283.

Beurel E, and Jope R, (2006). The paradoxical pro- and anti-apoptotic actions of GSK3 in the intrinsic and extrinsic apoptosis signaling pathways. *Progress in Neurobiology* **79**: 173–189.

Blann A, and Lip G, (2000). Cell Adhesion Molecules in Cardiovascular Disease and Its Risk Factors—What Can Soluble Levels Tell Us? *Journal of Clinical Endocrinology* **85**: 175-1747.

Blot W, and McLaughlin J, (1999). The changing epidemiology of esophageal cancer. *Seminars in Oncology* **5**: S2-S8.

Bramhall S, Noack N, Wu M, and Loewenberg J, (1969). A simple colorimetric method for determination of protein. *Analytical Biochemistry* **31**: 146-148.

Brodsky B, and Persikov A, (2005). Molecular structure of the collagen triple helix. *Advances in Protein Chemistry* **70**: 301–339.

Brunelle J, and Letai A, (2009). Control of mitochondrial apoptosis by the Bcl-2 family. *Journal of Cell Science* **122**: 437-441.

Cai G, Wang J, Xin X, Ke Z, and Luo J, (2007). Phosphorylation of glycogen synthase kinase-3 ß at serine 9 confers cisplatin resistance in ovarian cancer cells. *International Journal of Oncology* **31**: 657–662.

Campbell I, and Humphries M, (2011). Integrin structure, activation, and interactions. *Cold Spring Harbor Perspectives in Biology* **3**: a004994.

Chen H, and Guan J, (1994). Association of focal adhesion kinase with its potential substrate phosphatidylinositol 3-kinase. *Proceedings of the National Academy of Sciences* **91**: 10148–10152.

Chiarugi P, (2008). From anchorage dependent proliferation to survival: Lessons from redox signalling. *International Union of Biochemistry and Molecular Biology Life* **60**: 301–307.

Chuang D, Wang Z, and Chiu C, (2011). GSK-3 as a target for lithium-induced neuroprotection against excitotoxicity in neuronal cultures and animal models of ischemic stroke. *Frontiers in Molecular Neuroscience* **4**: 15.

Cohen P, and Frame S, (2001). The renaissance of GSK3. *Nature Reviews Molecular and Cell Biology* **2**: 769–776.

Cox T, and Erler J, (2011). Remodeling and homeostasis of the extracellular matrix: implications for fibrotic diseases and cancer. *Disease Models & Mechanisms* **4**: 165-178.

Cross D, Alessi D, Cohen P, Andjelkovich M, and Hemmings B, (1995). Inhibition of glycogen synthase kinase-3 by insulin mediated by protein kinase B. *Nature* **378**: 785-789.

DeNardo D, Brennan D, Rexhepaj E, Ruffell B, Shiao S, Madden S, Gallagher W, Wadhwani N, Keil S , Junaid S, Rugo H, Hwang E, Jirström K, West B, and Coussens L, (2011). Leukocyte complexity predicts breast cancer survival and functionally regulates response to chemotherapy. *Cancer Discovery* **1**: 54–67.

Desgrosellier J, Barnes L, Shields D, Huang M, Lau S, Prévost N, Tarin D, Shattil S, and Cheresh D, (2009). An integrin alpha(v)beta(3)-c-Src oncogenic unit promotes anchorage-independence and tumor progression. *Nature Medicine* **15**: 1163–1169.

Desgrosellier J, and Cheresh D, (2010). Integrins in cancer: biological implications and therapeutic opportunities. *Nature Reviews Cancer* **10**: 9–22.

Dickinson D, Nelson W, and Weis W, (2011). A polarized epithelium organized by beta- and alpha-catenin predates cadherin and metazoan origins. *Science* **331**: 1336─1339.

Elzey B, Griffith T, Herndon J, Barreiro R, Tschopp J, and Ferguson T, (2001). Regulation of Fas ligand-induced apoptosis by TNF. *Journal of Immunology* **167**: 3049-3056.

Fernald K, and Kurokawa M, (2013). Evading apoptosis in cancer. *Trends in Cell Biology* **23**: 620-633.

Frame S, and Cohen P, (2001). GSK3 takes centre stage more than 20 years after its discovery. *Biochemical Journal* **359**: 1.

Frisch M, and Francis H, (1994). Disruption of epithelial cell-matrix interactions induces apoptosis. *Journal of Cell Biology* **124**: 619–626.

Frost V, Al-Mehairi S, and Sinclair A, (2001). Exploitation of a non-apoptotic caspase to regulate the abundance of the cdkI p27(KIP1) in transformed lymphoid cells. *Oncogene* **20**: 2737–2748.

Fu Y, Wang X, Cheng X, Ye F, Xie X, and Lu W, (2014). Clinicopathological and biological significance of aberrant activation of glycogen synthase kinase-3 in ovarian cancer. *OncoTargets and Therapy* **7**: 1159-1168.

Gao C, Chen G, Kuan S, Zhang D, Schlaepfer D, and Hu J, (2015). FAK/PYK2 promotes the Wnt/β-catenin pathway and intestinal tumorigenesis by phosphorylating GSK3β. *eLife* **4**: e10072.

Gimenez-Bonafe P, Tortosa A, Perez-Tomas R, (2009). Overcoming drug resistance by enhancing apoptosis of tumor cells. *Current Cancer Drug Targets* **9**: 320–340.

Guerin R, Arseneault G, Dumont S, Rokeach A, (2008). Calnexin is involved in apoptosis induced by endoplasmic reticulum stress in the fission yeast. *Molecular Biology of the Cell* **19**: 4404–4420.

Gumbiner B, (1996) Cell adhesion: the molecular basis of tissue architecture and morphogenesis. *Cell* **84**: 345–357.

Hanahan D, and Weinberg R, (2011). Hallmarks of cancer: the next generation. *Cell* **144**: 646-674.

Hou S, Hang Q, Isaji T, Lu J, Fukuda T, and Gu J, (2016). Importance of membrane-proximal N-glycosylation on integrin β1 in its activation and complex formation. *FASEB Journal* **30**: 4120-4131.

Huang Q, Li F, Liu X, Li W, Shi W, Liu F, O'Sullivan B, He Z, Peng Y, Tan A, Zhou L, Shen J, Han G, Wang X, Thorburn J, Thorburn A, Jimeno A, Raben D, Bedford J, and Li C, (2011). Caspase 3–mediated stimulation of tumor cell repopulation during cancer radiotherapy. *Nature Medicine* **17**: 860–866.

Humphries J, (2006). Integrin ligands at a glance. *Journal of Cell Science* **119**: 3901-3903.

Humphries M, (2009). Cell adhesion assays. *Methods in Molecular Biology* **522**: 203-210.

Iitaka D, Moodley S, Shimizu H, Bai X, and Liu M, (2015). PKCδ–iPLA2–PGE2–PPARγ signaling cascade mediates TNF-α induced Claudin 1 expression in human lung carcinoma cells.

Jope R, Yuskaitis C, and Beurel E, (2007). Glycogen Synthase Kinase-3 (GSK3): Inflammation, Diseases, and Therapeutics. *Neurochemical Research* **32**: 577-595.

Kang Y, Digicaylioglu M, Russo R, Kaul M, Achim C, Fletcher L, Masliah E, and Lipton S, (2010). Erythropoietin plus insulin-like growth factor-I protects against neuronal damage in a murine model of human immunodeficiency virus-associated neurocognitive disorders. *Annals of Neurology* **68**: 342-352.

Ko Y, Cho S, Park J, Choi Y, Lee J, and Youn H, (2016). Hypoxic inactivation of glycogen synthase kinase-3 promotes gastric tumor growth and angiogenesis by facilitating hypoxia-inducible factor-1 signaling. *APMIS* **124**: 748–756.

Korur S, Huber R, Sivasankaran B, Petrich M, Morin Jr P, Hemmings B, Merlo A, and Lino M, (2008). GSK3β Regulates Differentiation and Growth Arrest in Glioblastoma. *PLoS ONE* **4**: e7443.

Kotliarova S, Pastorino S, Kovell L, Kotliarov Y, Song H, Zhang W, Bailey R, Maric D, Zenklusen J, Lee J, and Fine H, (2008). Glycogen Synthase Kinase-3 Inhibition Induces Glioma Cell Death through c-MYC, Nuclear Factor-κB, and Glucose Regulation. *Cancer Research* **68**: 6643-6650.

Laemmli U, (1970). Cleavage of structural proteins during the assembly of the head of bacteriophage T4. *Nature* **227**: 680-685.

Lang C, Hrdliczka E, Schweiger T, Glueck O, Lewik G, Schwarz S, Benazzo A, Lang G, Plepetko W, and Hoetzenecker K, (2017). Impact of cyclooxygenase-2 and prostaglandin-E2 expression on clinical outcome after pulmonary metastasectomy. *Journal of Thoracic Disease* **9**: 10612.

Läubli H, and Borsig L, (2019). Altered Cell Adhesion and Glycosylation Promote Cancer Immune Suppression and Metastasis. *Frontiers in Immunology* **10**: 2120.

Leber B, Lin J, and Andrews D, (2007). Embedded together: the life and death consequences of interaction of the Bcl-2 family with membranes. *Apoptosis* **12**: 897-911.

Lee J, and Streuli C, (2014). Integrins and epithelial cell polarity. *Journal of Cell Science* **127**: 3217-3225.

Lee Y, Jin J, Cheng C, Huang C, Song J, Huang M, Brown W, Zhang S, Yu-Lee L, Yeh E, McIntyre B, Logothetis C, Gallick G, and Lin S, (2013). Targeting constitutively activated β_1 integrins inhibits prostate cancer metastasis. *Molecular Cancer Research* **11**: 405–417.

Legate K, and Fässler R, (2009). Mechanisms that regulate adaptor binding to β-integrin cytoplasmic tails. *Journal of Cell Science* **122**: 187–198.

Letai A, Bassik M, Walensky L, Sorcinelli M, Weiler S, and Korsmeyer S, (2002). Distinct BH3 domains either sensitize or activate mitochondrial apoptosis, serving as prototype cancer therapeutics. *Cancer Cell* **2**: 183-192.

Li S, Edgar D, Fässler R, Wadsworth W, and Yurchenco P, (2003). The Role of Laminin in Embryonic Cell Polarization and Tissue Organization. *Developmental Cell* **4**: 613-624.

Li P, Nijhawan D, Budihardjo I, Srinivasula S, Ahmad M, Alnemri E, and Wang X, (1997). Cytochrome c and dATP-dependent formation of Apaf-1/caspase 9 complex initiates an apoptotic protease cascade. *Cell* **91**: 479-489.

Li J, Yang Z, Ren X, Zou Q, Yuan Y, Liang L, Chen M, and Chen S, (2012). ILK and PRDX1 are prognostic markers in squamous cell/adenosquamous carcinomas and adenocarcinoma of gallbladder. *Tumor Biology* **34**: 359-368.

Liao Y, Zhang Z, Zhao J, and Liu J, (2018). Effects of fibronectin 1 on cell proliferation, senescence and apoptosis of human glioma cells through the PI3K/AKT signaling pathway. *Cellular Physiology and Biochemistry* **48**: 1382–1396.

Lin E, Karakasheva T, Hicks P, Bass A, and Rustgi A, (2016). The Tumor Microenvironment in Esophageal Cancer. *Oncogene* **35**: 5337–5349.

Linding R, Jensen L, Ostheimer G, van Vugt M, Jørgensen C, Miron I, Diella F, Colwill K, Taylor L, Elder K, Metalnikov P, Nguyen V, Pasculescu A, Jin J, Park J, Samson L, Woodgett J, Russell R, Bork P, Yaffe M, and Pawson T, (2007). Systematic discovery of in vivo phosphorylation networks. *Cell* **129**: 1415-1426.

Locksley R, Killeen N, and Lenardo M, (2001). The TNF and TNF receptor superfamilies: integrating mammalian biology. *Cell* **104**: 487-501.

Luengo A, Gui D, and Heiden M, (2017). Targeting metabolism for cancer therapy. *Cell Chemical Biology* **24**: 1161–1180.

Macara I, and McCaffrey L, (2013). Cell polarity in morphogenesis and metastasis. *Philosophical Transactions of the Royal Society B: Biological Sciences* **368**: 12.

Mao Y, and Schwarzbauer J, (2005). Fibronectin fibrillogenesis, a cell-mediated matrix assembly process. *Matrix Biology* **24**: 389–399.

Martin S, Janouskova H, and Dontenwill M, (2012). Integrins and p53 pathways in glioblastoma resistance to temozolomide. *Frontiers in Oncology* **2**: 157.

Maydan M, McDonald P, Sanghera J, Yan J, Rallis C, Pinchin S, Hannigan G, Foster L, Ish-Horowicz D, Walsh M, and Dedhar S (2010). Integrin-linked kinase is a functional Mn2+-dependent protein kinase that regulates glycogen synthase kinase-3beta (GSK-3beta) phosphorylation. *PLoS ONE* **5**: e12356.

McDonald P, Fielding A, and Dedhar S, (2008). Integrin-linked kinase - essential roles in physiology and cancer biology. *Journal of Cell Science* **121**: 3121-3132.

Mirlashari M, Randen I, and Kjeldsen-Kragh J, (2012). Glycogen synthase kinase-3 (GSK-3) inhibition induces apoptosis in leukemic cells through mitochondria-dependent pathway. *Leukemia Research* **36**: 499–508.

Mosmann T, (1983). Rapid colorimetric assay for cellular growth and survival: application to proliferation and cytotoxicity assays. *Journal of Immunological Methods* **65**: 55–63.

Nam J, Ahmed K, Costes S, Zhang H, Onodera Y, Olshen A, Hatanaka K, Kinoshita R, Ishikawa M, Sabe H, Shirato H, and Park C, (2013). β1-Integrin via NF-κB signaling is essential for acquisition of invasiveness in a model of radiation treated in situ breast cancer. *Breast Cancer Research* **15**: 60.

Naylor M, Li N, Cheung J, Lowe E, Lambert E, Marlow R, Wang P, Schatzmann F, Wintermantel T, and Schüetz G, (2005). Ablation of beta1 integrin in mammary epithelium reveals a key role for integrin in glandular morphogenesis and differentiation. *Journal of Cell Biology* **171**: 717–728.

Novak A, Hsu S, Leung-Hagesteijn C, Radeva G, Papkoff J, Montesano R, Roskelley C, Grosschedl R, and Dedhar S, (1998). Cell adhesion and the integrin-linked kinase regulate the LEF-1 and β-catenin signaling pathways. *Proceedings of the National Academy of Sciences* **95**: 4374–4379.

Okegawa T, Pong R, Li Y, and Hseih J, (2004). The role of cell adhesion molecule in cancer progression and its application in cancer therapy. *Acta Biochimica Polonica* **51**: 445–457.

Oloumi A, McPhee T, and Dedhar S, (2004). Regulation of E-cadherin expression and beta-catenin/Tcf transcriptional activity by the integrin-linked kinase. *Biochimica et Biophysica Acta* **1691**: 1–15.

Pan B, Guo J, Liao Q, and Zhao Y, (2018). β1 and β3 integrins in breast, prostate and pancreatic cancer: A novel implication. *Oncology Letters* **15**: 5412–5416.

Pankov R, and Yamada K, (2002). Fibronectin at a glance. *Journal of Cell Science* **115**: 3861–3863.

Parton M, Krajewski S, Smith I, Krajewska M, Archer C, Naito M, Ahern R, Reed J, and Dowsett M, (2002). Coordinate expression of apoptosis-associated proteins in human breast cancer before and during chemotherapy. *Clinical Cancer Research* **8**: 2100-2108.

Paszek M, Zahir N, Johnson K, Lakins J, Rozenberg G, Gefen A, Reinhart-King C, Margulies S, Dembo M, Boettiger D, Hammer D, and Weaver V, (2005). Tensional homeostasis and the malignant phenotype. *Cancer Cell* **8**: 241–254.

Persad S, Attwell S, Gray V, Delcommenne M, Troussard A, Sanghera J, and Dedhar S, (2000). Inhibition of integrin-linked kinase (ILK) suppresses activation of protein kinase B/Akt and induces cell cycle arrest and apoptosis of PTEN-mutant prostate cancer cells. *Proceedings of the National Academy of Sciences* **97**: 3207-3212.

Plati J, Bucur O, and Khosravi-Far R, (2008). Dysregulation of Apoptotic Signaling in Cancer: Molecular Mechanisms and Therapeutic Opportunities. *Journal of Cellular Biochemistry* **104**: 1124-1149.

Popov C, Radic T, Haasters F, Prall W, Aszodi A, Gullberg D, Schieker M, and Docheval D, (2011). Integrins α2β1 and α11β1 regulate the survival of mesenchymal stem cells on collagen I. *Cell Death & Disease* **2**: e186.

Ramaswamy S, Ross K, Lander E, and Golub T, (2003) A molecular signature of metastasis in primary solid tumors. Nature Genetics **33**: 49–54.

Rooney N, and Streuli C, (2011). How integrins control mammary epithelial differentiation: A possible role for the ILK-PINCH-Parvin complex. *FEBS Letters* **585**: 1663-1672.

Rudnick J, and Kuperwasser C, (2012). Stromal biomarkers in breast cancer development and progression. *Clinical and Experimental Metastasis* **29**: 663–672.

Sakahira H, Enari M, and Nagata S, (1998). Cleavage of CAD inhibitor in CAD activation and DNA degradation during apoptosis. *Nature* **391**: 96-99.

Salvesen G and Riedl S, (2009). A conditional death domain complex mediating signaling by receptor clustering. *Cell Cycle* **8**: 2723-2727.

Schaller M D, Hildebrand J, Shannon J, Fox J, Vines R, and Parsons J, (1994). Autophosphorylation of the focal adhesion kinase, pp125FAK, directs SH2- dependent binding of pp60src. *Molecular Cell Biology* **14**: 1680–1688.

Schimmer A, (2004). Inhibitor of apoptosis proteins: translating basic knowledge into clinical practice. *Cancer Research* **64**: 7183-7190.

Schimmer A, Dalili S, Batey R, and Riedl S, (2006). Targeting XIAP for the treatment of malignancy. *Cell Death and Differentiation* **13**: 179–188.

Schneider C, Rasband W, and Eliceiri K, (2012). NIH Image to ImageJ: 25 years of image analysis. *Nature Methods* **9**: 671–675.

Shamas-Din A, Kale J, Leber B, and Andrews D, (2013). Mechanisms of Action of Bcl-2 Family Proteins. *Cold Spring Harbor Perspectives in Biology* **5**: a008714.

Shattil S, Kim C, and Ginsberg M, (2010). The final steps of integrin activation: the end game. *Nature Reviews Molecular Cell Biology* **11**: 288–300.

Siera O, and del Rio J, (2014). Glycogen synthase kinase 3 beta (GSK3β) at the tip of neuronal development and regeneration. *Molecular Neurobiology* **49**: 931–944.

St Johnston D, and Ahringer J, (2010). Cell Polarity in Eggs and Epithelia: Parallels and Diversity. *Cell* **141**: 757-774.

Sun M, Song L, Li Y, Zhou T, and Jope R, (2008). Identification of an antiapoptotic protein complex at death receptors. *Cell Death and Differentiation* **15**: 1887–1900.

Towbin H, Staehelin T, and Gordon J, (1979). Electrophoretic transfer of proteins from polyacrylamide gels to nitrocellulose sheets: procedure and some applications. *Proceedings of the National Academy of Sciences* **76**: 4350-4354.

Trigos A, Pearson R, Papenfuss A, and Good A, (2018). How the evolution of multicellularity set the stage for cancer. *British Journal of Cancer* **118**: 145─152.

Uliasz T, and Hewett S, (2000). A microtiter trypan blue absorbance assay for the quantitative determination of excitotoxic neuronal injury in cell culture. *Journal of Neuroscience Methods* **100**: 157–163.

Underwood T, Derouet M, White M, Noble F, Moutasim K, Smith E, Drew P, Thomas G, Primrose J, and Blaydes J, (2010) A comparison of primary oesophageal squamous epithelial cells with HET-1A in organotypic culture. *Biology of the Cell* **102**: 635-644.

Vanderslice P, and Woodside D, (2006). Integrin antagonists as therapeutics for inflammatory diseases. *Expert Opinion on Investigational Drugs* **15**: 1235-1255.

Veale R, and Thornley A, (1989). Increased single class low-affinity EGF receptors expressed by human oesophageal squamous carcinoma cell lines. *South African Medical Journal of Science* **85**: 375-379.

Wang J, and Hielscher A, (2017). Fibronectin: How Its Aberrant Expression in Tumors May Improve Therapeutic Targeting. *Journal of Cancer* **8**: 674-682.

Woods N, Muessig A, Schmidt M, Flygare J, Olsson K, Salmon P, Trono D, von Kalle C, and Karlsson S, (2003). Lentiviral vector transduction of NOD/SCID repopulating cells results in multiple vector integrations per transduced cell: risk of insertional mutagenesis. *Blood* **101**: 1284–1289.

Wu G, Huang H, Abreu J, and He X, (2009). Inhibition of GSK3 Phosphorylation of β-Catenin via Phosphorylated PPPSPXS Motifs of Wnt Coreceptor LRP6. *PLoS ONE* **4**: e4926.

Wu S, Zhu W, Thompson P, and Hannun Y, (2018). Evaluating intrinsic and non-intrinsic cancer risk factors. *Nature Communications* **9**: 3490.

Wu W, Wu J, and Hu C, (2008). Signal cross talks for sustained MAPK activation and cell migration: the potential role of reactive oxygen species. *Cancer and Metastasis Reviews* **27**: 303–317.

Xu Z, Zou L, Ma G, Wu X, Huang F, Feng T, Li S, Lin Q, He X, Liu Z, and Cao X, (2017). Integrin β1 is a critical effector in promoting metastasis and chemo-resistance of esophageal squamous cell carcinoma. *American Journal of Cancer Research* **7**: 531–542.

Yoshino Y, and Ishioka C, (2015). Inhibition of glycogen synthase kinase-3 beta induces apoptosis and mitotic catastrophe by disrupting centrosome regulation in cancer cells. *Scientific Reports* **4**: 13249.

Zeng J, Liu D, Qiu Z, Huang Y, Chen B, Wang L, Xu H, Huang N, Liu L, and Li W, (2014). GSK3β overexpression indicates poor prognosis and its inhibition reduces cell proliferation and survival of non-small cell lung cancer cells. *PLoS ONE* **9**: e91231.

Zhang Y, (2013). Epidemiology of esophageal cancer. *World Journal of Gastroenterology* **19**: 5598.

Zheng W, Gu X, Sun X, Wu Q, and Dan H, (2019). FAK mediates BMP9-induced osteogenic differentiation via Wnt and MAPK signaling pathway in synovial mesenchymal stem cells. *Artificial Cells, Nanomedicine, and Biotechnology* **47**: 2641–2649.

APPENDIX A

1. Tissue culture

1.1 Phosphate-buffered saline (1×)

136.9 mM Sodium Chloride

2.68 mM Potassium Chloride

10.1 mM Disodium Hydrogen Phosphate Dodecahydrate

1.76 mM Potassium Dihydrogen Phosphate

Make up to volume with dH_2O

Adjust pH to 7.2 - 7.3

Autoclave to sterilise

Store at 4ºC

1.2 Trypsin/EDTA

0.02% EDTA in 500 mL PBS

0.1% Trypsin in 1 L PBS

Mix EDTA and trypsin in 1:1 ratio

Store at 4ºC

1.3 Tissue culture medium

1.3.1 Dulbecco's Modified Eagles Medium

1.37% DMEM

0.37% Sodium Bicarbonate

2% 500 U/mL Penicillin and 0.5 % Streptomycin Solution

1.3.2 Hams F12 nutrient mixture

1.07% Hams F12 Medium

0.118% Sodium Bicarbonate

2% 500 U/mL Penicillin and 0.5% Streptomycin Solution

1.3.3 DMEM/Hams F12 Medium Solution

Mix DMEM and Hams F12 nutrient mixture in a 3:1 ratio

Filter sterilise

Store at 4℃

2. Growth on extracellular matrix

2.1 Collagen type I as substrate

2.1.1 Collagen type I stock solution

3 mg/mL Rat Tail Collagen

Make up to volume with 0.5 M acetic acid

2.1.2 Collagen type I working solution

100 µg/mL Collagen I Stock Solution

Make up to volume with 0.02 N acetic acid

2.2 Fibronectin as substrate

2.2.1 Fibronectin stock solution

1 mg/mL Fibronectin (Roche)

Prepare in sterile PBS

2.2.2 Fibronectin working solution

10 µg/mL Fibronectin Stock Solution

Make up to volume with sterile PBS

3. Whole-cell protein extraction

3.1 PMSF stock solution

20 mM PMSF (Sigma-Aldrich)

Make up to volume with methanol

Store at 4℃

3.2 Double Laemmli lysis buffer

125 mM Tris-HCl (pH 6.8)

4% SDS

20% Glycerol

10% β-Mercaptoethanol

Make up to volume with dH_2O

Store at 4℃

3.3 BSA stock solution

0.1% BSA (Sigma-Aldrich)

Prepare in double Laemmli lysis buffer

Store at 4℃

3.4 Trichloroacetic acid

7.5% TCA

Make up to volume with dH_2O

3.5 Coomassie Brilliant Blue stain

0.25% Coomassie Brilliant Blue powder

50% Methanol

10% Glacial Acetic Acid

Make up to volume with dH_2O

Store at room temperature

3.6 Destain

12% Glacial Acetic Acid

10% Methanol

Make up to final volume with dH_2O

3.7 Elution solution

66% Methanol

33% Deionised water

1% Concentrated Ammonia

Store at room temperature

4. SDS-PAGE

4.1 SDS solution

50 mg/mL SDS

Make up to volume with dH_2O

Agitate to facilitate dissolution

Store at room temperature

4.2 Separating gel

4.2.1 Separating buffer

375 mM Tris-HCl

Adjust pH to 8.8

Make up to volume with dH_2O

4.2.2 Separating gel solution (10%)

10% Acrylamide

25% Separating Buffer

4% SDS Solution

4% NN'-Methylenebisacrylamide Solution

Make up to volume with dH_2O

Immediately before use add:

1.8% 0.05 M Ammonium Persulphate (APS) Solution

0.25% N,N,N',N'-Tetramethylenediamine (TEMED)

4.3 Stacking gel

4.3.1 Stacking buffer

125 mM Tris-HCl

Adjust pH to 6.8

Make up to final volume with dH_2O

4.3.2 Stacking gel solution (5%)

5% Acrylamide

25% Stacking Buffer

4% SDS Solution

4% NN'-Methylenebisacrylamide Solution

Make up to final volume with dH_2O

Immediately before use add:

1.8% 0.05 M APS Solution

0.25% TEMED

4.4 SDS overlay solution

400µL of 50mg/mL SDS Solution

Make up to volume with dH_2O

4.5 SDS-PAGE running buffer

25 mM Tris-HCl

192.5 mM Glycine

3.74 mM SDS

Make up to volume with dH_2O

Store at room temperature

4.6 Coomassie Brilliant Blue stain

As described in Appendix 4.5

4.7 Destain

10% Glacial Acetic Acid

10% Methanol

Make up to volume with dH_2O

Store at room temperature

5. Western immunoblotting

5.1 Tris-buffered saline (1×)

50 mM Tris-HCl

147 mM Sodium Chloride

2 mM Anhydrous Calcium Chloride

Adjust pH to 7.8

Make up to volume with dH_2O

Autoclave to sterilise

Store at 4℃

5.2 Tris-buffered saline with Tween-20

10% TBS

0.1% Tween-20

Make up to volume with dH_2O

Store at 4℃

5.3 Transfer buffer

25 mM Tris-HCl

20% Methanol

188 mM Glycine

Adjust pH to 8.3

Make up to volume with dH_2O

5.4 Blocking solution

5% Non-Fat Dried Milk Powder

Make up to volume with TBS-T

5.5 Developing solution

6.4 M Metol

0.6 M Anhydrous Sodium Sulphate

80 mM Hydroquinone (Quinol)

0.45 mM Anhydrous Sodium Carbonate

34 mM Potassium Bromide

Make up to volume with dH_2O

Store at room temperature in the dark

5.6 Fixing solution

0.8 M Sodium Thiosulphate

0.2 M Sodium Metasulphite

Make up to volume with dH_2O

Store at room temperature in the dark

6. MTT cell proliferation assay

6.1 MTT working solution

0.25 mg/mL MTT tetrazolium dye

Make up to volume in fresh 3:1 DMEM/Hams F12 tissue culture medium

7. Crystal violet cell adhesion assay

7.1 Crystal violet stain (0.5%)

0.5 g Crystal violet powder

20 mL Methanol

80 mL dH_2O

Mix crystal violet powder with dH_2O and dissolve

Add methanol

Store at room temperature in the dark

8. Trypan Blue cell viability assay

8.1 Trypan Blue solution (0.4%)

4 mg Trypan Blue powder

Make up to volume with sterile PBS

Filter sterilise

Store at 4ºC

8.2 SDS solution (1%)

1 g SDS

Make up to volume with dH_2O

Store at room temperature

APPENDIX B

1. Example of standard curve used for the quantitative estimation of protein concentration of the whole-cell lysates

In order to ensure equal loading of whole-cell protein lysates on subsequent SDS-PAGE gels, quantitative estimation of protein concentration was performed as per the modified protocol of Bramhall *et al.* (1969). A standard curve was constructed to calculate the protein concentration from the obtained absorbencies. A representative standard curve is indicated in Figure B1.

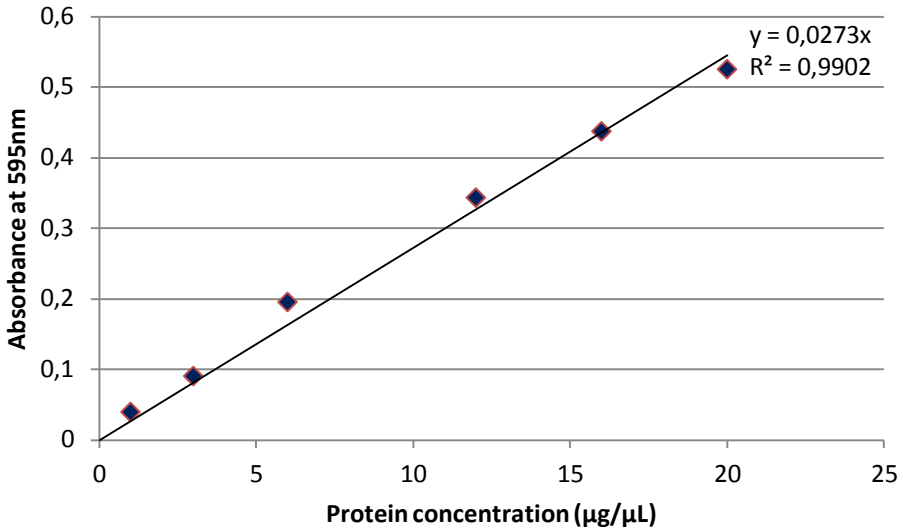

Figure B1. Example standard curve for quantitative estimation of protein concentration.

To construct a standard curve to quantitatively estimate the protein concentrations of each respective whole-cell extract obtained from the five HOSCC cell lines, and H1299 control cell line, the absorbencies of 1, 3, 6, 12, 16, and 20 µg/µL of BSA in double Laemmli lysis buffer were measured at 595 nm. Determination of protein concentration was carried out using the constructed BSA standard curve ($y = 0.0273x$; $R^2 = 0.9902$) and the absorbencies of the whole-cell extracts at 595 nm.

2. Example of 10% (w/v) SDS-PAGE gel used to separate and resolve the whole-cell extacts

A 10% (w/v) reducing, discontinuous SDS-PAGE gel was employed in order to resolve and separate the target protein set prior to immunodetection by Western immunoblotting. A representative SDS-PAGE gel indicating the separation of the whole-cell protein extracts is shown in Figure B2.

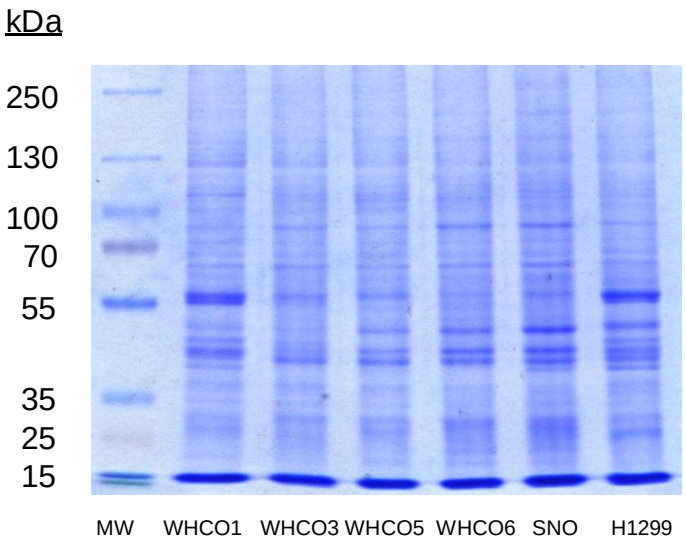

Figure B2. Electrophoretic separation of whole cell extracts on a 10 % (w/v) reducing SDS-PAGE gel.

A representative 10 % (w/v) polyacrylamide gel was prepared and whole-cell lysates extracted from five moderately differentiated HOSCC cell lines were separated using discontinuous, reducing SDS-PAGE. A prestained, low molecular weight marker was loaded into the first lane to observe relative molecular weights in kDa. Approximately 5 µg of each whole cell extract was loaded into each lane, as indicated by a consistent level of staining.

3. Antibodies used for western immunoblotting

Table B1. Concentrations of antibodies used for the immunodetection of the target protein set during western immunoblotting.

Antibody	Concentration	Diluent	Manufacturer
Mouse polyclonal anti-β1 integrin primary antibody	1:10 000	2.5% milk TBS-T	Merck, SA
Rabbit polyclonal anti-pGSK3β (Tyr-216) primary antibody	1:2 000	2.5% BSA TBS-T	Abcam, UK
Rabbit polyclonal anti-pGSK3β (Ser-9) primary	1:1 000	2.5% BSA TBS-T	Cell Signaling Technology, USA
Rabbit polyconal anti-caspase 3 primary antibody	1:500	PBS	Santa Cruz Biotechnology, USA
Rabbit polyclonal anti-β-actin primary antibodies	1:2 500	2.5% milk PBS	Cell Signaling Technology, USA

3. Tables of data

Table B2. Raw densitometric data of baseline western immunoblots using ImageJ allowed for semi-quantitative analysis of the relative abundance of protein levels in HOSCC.

As a reflection of the sensitivity of the detection of optical densities in the Western immunoblots by ImageJ, as well as to maintain consistency, all data were rounded to three significant figures. All densitometric data was obtained in triplicate. Note: IOD = Integrated Optical Density, SEM = Standard Error of the Mean.

Protein	**Cell line**											
	WHCO1		**WHCO3**		**WHCO5**		**WHCO6**		**SNO**		**H1299**	
	IOD	**SEM**	**IOD**	**SEM**	**IOD**	**SEM**	**IOD**	**SEM**	**IOD**	**SEM**	**IOD**	**SEM**
β1 integrin	0.87 0.72 1.60	0.06	0.27 0.29 0.49	0.09	0.52 0.24 0.49	0.11	0.60 0.55 0.84	0.02	0.62 0.99 0.65	0.01	1.00 1.00 1.00	0.00
pGSK3β (Tyr-216)	0.44 0.41 0.66	0.09	0.83 0.78 0.44	0.16	0.19 0.23 0.14	0.02	0.57 0.76 0.87	0.12	0.87 0.43 0.70	0.07	1.00 1.00 1.00	0.00
pGSK3β (Ser-9)	0.79 0.78 0.68	0.09	1.06 0.87 0.84	0.12	0.94 0.59 0.73	0.14	1.16 0.68 1.17	0.18	0.82 0.83 0.49	0.11	1.00 1.00 1.00	0.00
Cleaved caspase 3	0.50 0.57 0.67	0.07	0.36 0.34 0.55	0.08	0.48 0.60 0.44	0.05	0.87 0.93 0.48	0.02	0.82 0.73 0.67	0.04	1.00 1.00 1.00	0.00
β-actin	1.07	N/A	0.94	N/A	0.96	N/A	0.97	N/A	1.16	N/A	1.00	N/A

Table B3. Raw data for baseline Crystal Violet cell adhesion assays, MTT cell proliferation assays, and Trypan Blue cell viability assays.

Cell line	Crystal Violet cell adhesion assay		MTT cell proliferation assay		Trypan Blue cell viability assay	
	A_{570}	SEM	A_{570}	SEM	A_{590}	SEM
WHCO1	0.82 0.98 0.67	0.06	1.36 1.17 1.54	0.08	0.72 0.98 0.43	0.08
WHCO3	0.97 0.80 1.16	0.23	1.53 1.55 1.43	0.05	0.66 0.71 0.61	0.05
WHCO5	1.13 0.89 1.14	0.09	0.81 0.84 0.69	0.02	0.92 1.26 1.08	0.07
WHCO6	1.05 1.10 0.89	0.02	1.34 1.41 1.27	0.03	0.52 0.46 0.59	0.05
SNO	0.86 0.81 0.73	0.09	0.72 0.81 0.63	0.08	0.83 0.74 1.12	0.05
H1299	1.00 1.00 1.00	0.00	1.00 1.00 1.00	0.00	1.00 1.00 1.00	0.00

(Note: A_{570} = Absorbencies obtained at 570 nm, A_{590} = Absorbencies obtained at 590 nm)

Table B4. Raw data for MTT cell proliferation assays, and Trypan blue cell viability assays performed on HOSCC cells following specific abrogation of GSK3β activity.

Cell line	Treatment	MTT cell proliferation assay		Trypan Blue cell viability assay	
		A_{570}	SEM	A_{590}	SEM
WHCO1	**NT**	1.44	0.08	0.12	0.01
		1.33		0.07	
		1.27		0.05	
	DMSO	1.40	0.17	0.11	0.01
		1.08		0.14	
		0.83		0.08	
	AR	2.04	0.05	0.10	0.01
		1.50		0.07	
		1.83		0.11	
WHCO5	**NT**	1.37	0.07	0.13	0.01
		1.26		0.12	
		1.33		0.10	
	DMSO	1.30	0.05	0.12	0.03
		0.82		0.14	
		0.82		0.12	
	AR	1.46	0.22	0.08	0.00
		1.28		0.09	
		1.27		0.09	
SNO	**NT**	1.58	0.24	0.16	0.00
		1.75		0.15	
		1.10		0.18	
	DMSO	1.18	0.17	0.12	0.00
		1.36		0.11	
		1.27		0.11	
	AR	2.16	0.16	0.15	0.00
		1.98		0.15	
		2.05		0.17	
H1299	**NT**	1.52	0.05	0.24	0.01
		1.51		0.18	
		1.47		0.23	
	DMSO	1.36	0.02	0.20	0.01
		1.32		0.21	
		1.39		0.20	
	AR	1.26	0.02	0.22	0.01
		1.24		0.25	
		1.18		0.21	

(Note: A_{570} = Absorbencies obtained at 570 nm, A_{590} = Absorbencies obtained at 590 nm, NT = Untreated, DMSO = DMSO-only control, AR = AR-A014418)

Table B5. Raw data for Crystal Violet cell adhesion assays, MTT cell proliferation assays, and Trypan Blue cell viability assays performed on HOSCC cells grown on an ECM-supplemented substrate.

Cell line	Condition	Crystal Violet cell adhesion assay		MTT cell proliferation assay		Trypan Blue cell viability assay	
		A_{570}	SEM	A_{570}	SEM	A_{590}	SEM
WHCO1	**NT**	0.86	0.23	1.20	0.17	0.26	0.01
		0.57		1.08		0.29	
		0.71		0.97		0.27	
	FN	0.57	0.08	1.06	0.17	0.25	0.00
		0.69		0.69		0.26	
		0.51		0.87		0.26	
	CN	0.36	0.02	0.94	0.13	0.49	0.03
		0.39		1.18		0.51	
		0.35		0.70		0.44	
WHCO5	**NT**	1.26	0.03	0.73	0.13	0.16	0.01
		1.15		0.66		0.18	
		1.36		0.69		0.17	
	FN	1.01	0.17	0.70	0.19	0.25	0.00
		0.89		0.85		0.26	
		0.85		1.16		0.25	
	CN	0.65	0.03	0.15	0.15	0.14	0.03
		0.61		0.22		0.18	
		0.57		0.26		0.14	
SNO	**NT**	1.89	0.01	0.64	0.17	0.08	0.00
		1.93		0.75		0.10	
		1.79		0.81		0.10	
	FN	1.66	0.08	0.60	0.11	0.15	0.00
		1.69		0.44		0.13	
		1.93		0.59		0.14	
	CN	1.57	0.16	1.05	0.13	0.10	0.00
		1.70		1.19		0.16	
		1.69		1.15		0.12	
H1299	**NT**	1.28	0.05	0.89	0.14	0.05	0.00
		1.13		0.97		0.07	
		1.26		0.86		0.07	
	FN	1.43	0.01	0.95	0.15	0.11	0.01
		1.54		0.87		0.15	
		1.55		1.19		0.13	
	CN	1.70	0.37	1.37	0.12	0.16	0.01
		1.98		1.22		0.17	
		2.01		1.14		0.20	

(Note: A_{570} = Absorbencies obtained at 570 nm, A_{590} = Absorbencies obtained at 590 nm, FN = Fibronectin, CN = Collagen type I)

Table B6. Raw densitometric data of western immunoblots using ImageJ allowed for semi-quantitative analysis of the relative abundance of protein levels in HOSCC following specific inhibition of GSK3β using the small molecule inhibitor AR-A014418.

As a reflection of the sensitivity of the detection of optical densities in the Western immunoblots by ImageJ, as well as to maintain consistency, all data were rounded to three significant figures. All densitometric data was obtained in triplicate. Note: IOD = Integrated Optical Density, SEM = Standard Error of the Mean.

Cell line	Treatment	β1 integrin		Cleaved caspase 3	
		IOD	**SEM**	**IOD**	**SEM**
WHCO1	**NT**	0.56 1.54 1.23	0.27	0.95 0.60 0.49	0.18
	DMSO	0.76 1.18 0.99	0.09	0.74 1.22 0.60	0.06
	AR	1.33 1.72 1.48	0.06	0.54 0.33 0.27	0.11
WHCO5	**NT**	0.67 0.70 0.59	0.03	0.35 0.21 0.17	0.07
	DMSO	0.65 0.82 0.73	0.02	1.28 0.70 0.64	0.26
	AR	1.43 1.32 0.88	0.22	1.66 1.06 0.83	0.34
SNO	**NT**	0.40 0.46 0.22	0.07	1.52 0.92 0.76	0.31
	DMSO	0.93 1.27 1.10	0.07	0.82 1.65 0.49	0.13
	AR	1.25 1.08 0.76	0.20	0.49 0.52 0.26	0.09
H1299	**NT**	0.86 1.15 0.91	0.02	0.76 0.85 0.79	0.01
	DMSO	0.77 0.62 0.37	0.16	0.84 0.63 0.59	0.10
	AR	0.65 0.84 1.52	0.35	0.44 0.23 0.12	0.13

(Note: NT = Untreated, DMSO = DMSO-only control, AR = AR-A014418)

Table B7. Raw densitometric data of western immunoblots using ImageJ allowed for semi-quantitative analysis of the relative abundance of protein levels in HOSCC following growth on collagen type I- or fibronectin-coated substrate.

As a reflection of the sensitivity of the detection of optical densities in the Western immunoblots by ImageJ, as well as to maintain consistency, all data were rounded to three significant figures. All densitometric data was obtained in triplicate. Note: IOD = Integrated Optical Density, SEM = Standard Error of the Mean.

Cell line	**Condition**	**pGSK3β (Ser-9)**	
		IOD	**SEM**
WHCO1	**NT**	1.14 1.26 1.18	0.01
	FN	1.65 1.87 1.53	0.04
	CN	0.55 0.72 0.66	0.04
WHCO5	**NT**	1.32 1.44 1.37	0.02
	FN	0.91 1.25 1.59	0.27
	CN	0.60 0.58 0.67	0.03
SNO	**NT**	0.85 1.12 0.95	0.04
	FN	1.59 1.48 1.66	0.02
	CN	1.98 2.06 2.01	0.01
H1299	**NT**	1.34 1.22 1.29	0.02
	FN	1.60 1.48 1.73	0.05
	CN	1.57 1.84 1.66	0.03

(Note: FN = Fibronectin, CN = Collagen type I)